PHILOSOPHICAL TRANSACTIONS OF THE ROYAL SOCIETY A MATHEMATICAL, PHYSICAL & ENGINEERING SCIENCES

Palaeosecular Variation Recorded by Lava Flows over the past Five Million Years

Catherine L. Johnson and Catherine G. Constable

Phil. Trans. R. Soc. Lond. A 1996 **354**, 89-141
doi: 10.1098/rsta.1996.0004

Palaeosecular variation recorded by lava flows over the past five million years

By Catherine L. Johnson† and Catherine G. Constable

Institute for Geophysics and Planetary Physics, Scripps Institution of Oceanography, La Jolla, CA 92093-0225, USA

Contents

We present a new global palaeomagnetic database, comprising lava flows and thin intrusive bodies, suitable for studying palaeosecular variation and the time-averaged field. The database is presented in some detail in the appendix and is available on-line from the authors. We review palaeosecular variation models to date, emphasizing the assumptions required and the rather arbitrary construction of many of these models. Preliminary studies of the statistical properties of the new database suggest that existing palaeosecular variation models are inadequate to explain the long-term temporal variations in the field. It is increasingly apparent that data distribution and quality are pivotal in determining the characteristics of the secular variation. The work presented here demonstrates the need for revised models of the time-averaged field structure for both normal and reverse polarities before reliable models for palaeosecular variation can be made.

---

† Present address: Carnegie Institution of Washington, Department of Terrestrial Magnetism, 5241 Broad Branch Road, N.W., Washington, DC, 20015, USA.

Phil. Trans. R. Soc. Lond. A (1996) **354**, 89–141
Printed in Great Britain

1. Introduction

(a) A new database for palaeosecular variation studies

Geomagnetic palaeosecular variation (PSV) describes the spatial and temporal variability of the field on time scales of 10^2–10^5 years, i.e. long-period variations of the field during stable polarity times. Long-period temporal variations are controlled by changes in the geodynamo which in turn may be controlled in part by conditions at the core–mantle boundary (CMB). PSV studies rely on remanent magnetizations retained by either archaeomagnetic materials or by sedimentary and igneous rocks, and are thus limited by the temporal and spatial distribution of data. Each of these three data sets has advantages and disadvantages. The remanence carried by archaeomagnetic materials and igneous rocks is primarily thermal in origin. It is acquired during cooling, either after firing of pottery or bricks, or after emplacement of igneous rocks. The remanence is thus acquired 'instantly' on geological timescales and provides a spot recording of the geomagnetic field direction. Archaeomagnetic data span only the past 10^3 years or so and provide no information on longer-period PSV. Igneous rocks provide secular variation information spanning periods of up to millions of years, but the data distribution is determined by the occurrence of volcanism and the present day accessibility of the lava flows. Sedimentary rocks have the advantage that a fairly continuous record of PSV can be obtained from specific locations if sedimentation has continued over a long period of time. The main disadvantages of sedimentary records are the temporal smoothing inherent in the remanence acquisition and the need for independent determinations of the sedimentation rate. Useful sedimentary records come from lakes and oceans, making these data expensive to acquire.

There have been many PSV studies reported over the past thirty years (see, for example, the summaries in Merrill & McElhinny (1983), McElhinny & Merrill (1975), and also the references for the database presented in this paper) but the data analysis methods used fall into two broad categories. In a few cases, it has been possible to examine continuous sedimentary records spanning the past 50 000 years using traditional time-series analysis approaches (see, for example, Creer *et al.* 1983). More commonly, PSV studies rely heavily on statistical approaches where the variance (dispersion) in the field is quantified in some way. The two most commonly used descriptions of PSV are the angular dispersion in the field directions or the angular dispersion in the virtual geomagnetic pole (VGP) positions. A VGP is computed assuming that the instantaneous field directions are due to a geocentric dipole.

In this paper we present an updated database, spanning the time interval 0–5 Ma, suitable for both studies of palaeosecular variation from lavas (PSVL) and time-averaged field modelling. We review previous PSV models, and their shortcomings, to place this database in context with previous work. We discuss briefly the time-averaged field problem and the need for improved estimates of the timescales for secular variation. Selection criteria for the new database are reported – the resulting database differs significantly from others used in PSVL work owing to these stringent selection criteria. A summary of the data is given in the appendix with a brief outline of each contributing study and stereographic plots of VGP positions divided according to geographical region. The distributions of VGP latitudes and longitudes are reported, together with a discussion of the relative contributions of normal and reverse polarity data. The data distributions are compared with the predictions of recent statistical models (Constable & Parker 1988; Egbert 1992). Angular dispersions in directions and in VGP positions have been computed for the past 5 Ma and

are compared with the results from more recent studies (McFadden *et al.* 1988, 1991) and with the predictions of the global statistical model (Constable & Parker 1988). We summarize the state of the art in PSV studies, relating the results to the revised database.

(*b*) *Palaeosecular variation models*

Over the past three decades, several models for PSV have been proposed which attempt to account for the angular dispersion observed in sedimentary and volcanic records. Traditionally, these models have attributed secular variation to three sources – variations in the intensity of the dipole part of the field, variations in the direction of the dipole (dipole wobble) and variations in the non-dipole field. Later statistical descriptions of palaeosecular variation have used present-day properties of the field to constrain the model; for example, McFadden *et al.* (1988) used the present-day field to establish the general form of a VGP dispersion curve, while Constable & Parker (1988) used the present-day power spectrum as a constraint on the palaeopower spectrum. It is important to note that none of these models were based on any physical theory: earlier models were based on the empirical observation that most of the power in the geomagnetic field observed at the earth's surface can be accounted for by a geocentric dipolar field structure, while later models were based on statistical properties of the field.

Models A (Irving & Ward 1964) and B (Creer *et al.* 1959; Creer 1962) considered only dipole wobble. Later models (model C (Cox 1962), model D (Cox 1970), model E (Baag & Helsley 1974), model M (McElhinny & Merrill 1975) and its modification (Harrison 1980), model F (McFadden & McElhinny 1984)) considered both dipole and non-dipole variations. These PSV models are defined by a set of statistical parameters describing the random variations in the non-dipole field, the dipole wobble (typically described by assuming the VGP distribution produced by the wobble is Fisherian with a specified angular dispersion) and the intensity variations. Many of the assumptions built into these models (for example, the form of the dipole intensity variations (Cox 1968)) are now known to be incorrect. Also important is the way in which the dipole wobble and non-dipole/dipole intensity parts of PSV are combined. This varies according to whether the total angular variance of the field directions or the VGPs is presumed to be Fisherian. Most studies have modelled the dispersion in VGPs rather than field directions since, first, the VGPs are generally assumed to have a more Fisherian distribution than the field directions, and, second, the VGP dispersion due to dipole wobble is latitude invariant, simplifying the analyses. Finally, correlations between the three sources of variations must be considered; for example, model F assumes that the non-dipole field intensity increases with the latitudinal increase in intensity of the axial dipole field. In addition to the large number of assumptions necessary in PSV models A, B, C, D, E, M and F, the distinction between dipole and non-dipole sources for PSV is purely mathematical rather than being based on physics.

Some of these concerns were recognized by McFadden *et al.* (1988), who put forward a different representation of PSV. Their model G invokes a result from dynamo theory, in which under certain conditions, the solution to the magnetohydrodynamic equations results in a magnetic field consisting of two independent families – the dipole family and quadrupole family. If these two families are independent, the total variance in the field is the sum of the variances due to the dipole family and the quadrupole family. The general form of the dispersion in the VGPs was established using the present-day field. It was found that the dispersion due to the quadrupole

PHILOSOPHICAL TRANSACTIONS OF THE ROYAL SOCIETY A MATHEMATICAL, PHYSICAL & ENGINEERING SCIENCES

family was constant with latitude, whereas the dispersion due to the dipole family varied linearly with latitude up to a latitude of 70°. At the equator, the contribution due to the variance from the dipole family is zero. McFadden *et al.* (1988) used this form for VGP dispersion to establish the dipole and quadrupole family contributions to SV over the past 5 Ma. McFadden *et al.* (1991) extended this study back to 195 Ma, with plate-motion corrections applied to data older than 5 Ma. Although this model is appealing because of its simplicity and possible interpretation in terms of a particular class of dynamo models, it is not clear whether the assumptions on which it is based are valid.

An alternative statistical approach was presented by Constable & Parker (1988), who considered the present-day spatial geomagnetic power spectrum to be a realization of a white-noise process near the CMB. Their description of PSV relies on the spherical-harmonic representation of the geomagnetic field, and allows the statistical variation in any palaeomagnetic data type to be predicted. In the Constable & Parker model, all the non-dipole spherical-harmonic coefficients (except for the axial quadrupole) of a given degree are identically independently distributed zero-mean Gaussian variables with a variance determined by the white spectrum at the CMB. Physically, this translates into temporal field variations with no average longitudinal dependence and the variance in each of the local orthogonal components of the field vector is independent of latitude. The dipole terms in the model have a lower variance than predicted using the spectrum at the CMB, and the axial dipole term has an expected magnitude specified by its present day value. The model also includes a non-zero mean axial quadrupole, in agreement with previous studies (see, for example, Wilson 1971; Creer *et al.* 1973; Merrill & McElhinny 1977; Livermore *et al.* 1983; Schneider & Kent 1990).

The Constable & Parker model (1988) illustrates a crucial assumption involved in the modelling of PSV, that of the structure of the time-averaged geomagnetic field. While it has been noted by several investigators that the time-averaged field can be approximated by an offset axial dipole, many applications of palaeomagnetism (for example, plate tectonics) rely on the assumption that over time the geomagnetic field can be described by a geocentric axial dipole (the GAD hypothesis). Most PSV studies have also assumed that the GAD hypothesis holds, so VGP dispersion is easily computed as the angular variance about the geographic pole. This assumption has been justified by the fact that small perturbations in the mean pole position have a very small effect on the calculated VGP dispersion (McFadden *et al.* 1988). Recent studies of reversal records (Tric *et al.* 1991; Clement *et al.* 1991; Laj *et al.* 1991) have suggested that there may be structure in the geomagnetic field, other than the axial dipole and axial quadrupole terms, with a longer timescale than PSV. The findings of these studies are currently under hot debate due to uncertainties associated with the fidelity of the reversal records and the rather small number of records available (Valet *et al.* 1992; Langereis *et al.* 1992; Laj *et al.* 1992; McFadden *et al.* 1993); however, the controversy surrounding the results is indicative of our lack of understanding of the long-period temporal variations in the field. It was suggested by Constable (1992) that the non-zonal field structure seen in some reversal records is also observed in the palaeosecular variation record. As we shall show, the new database presented here does not support this claim; however, the data do still appear to require non-zonal structure in the time-averaged field.

The most recent PSV studies (McFadden *et al.* 1988, 1991; McFadden & McElhinny 1984) have used a database comprising solely igneous rocks compiled by Lee (1983).

PHILOSOPHICAL TRANSACTIONS OF THE ROYAL SOCIETY A MATHEMATICAL, PHYSICAL & ENGINEERING SCIENCES

This database is a compilation of previously reported palaeomagnetic work, particularly from the 1970s, which was edited to be suitable for PSV studies. It comprises data spanning the past 195 Ma. Studies of the time-averaged field have used either sedimentary data alone (see, for example, Opdyke & Henry 1969; Schneider & Kent 1990) or combinations of sedimentary and igneous data (see, for example, Wilson 1971; Merrill & McElhinny 1977; Livermore *et al.* 1983, 1984; Merrill *et al.* 1990).

(*c*) *Problems with existing PSV models*

It can be seen that PSV studies are hindered by several factors, not least of all the current palaeomagnetic data distribution and our own preconceived notions concerning the behaviour of the geomagnetic field both temporally and spatially. We have noted that several models are based on the rather arbitrary separation of the field into dipole and non-dipole parts. Another model considers the secular variation to be due to two (assumed) independent sources – the dipole and quadrupole families. The majority of PSV studies have used VGP positions as the palaeomagnetic observable. Intuitively this seems reasonable as the major component of the field at the Earth's surface is the dipole term, and for a dipolar field it is simpler to think in terms of the VGP positions rather than the field directions. However, the VGP representation is also potentially confusing, especially for complex field structures, since the transformation between field directions and VGP positions is nonlinear. PSV dispersion analyses to date have assumed symmetry about the equator, even though this is not true for the present-day field and we will show that this assumption does not hold for PSV data over the past 5 Ma. Dispersion calculations require some knowledge of the time-averaged field structure, and although it is generally accepted that the time-averaged field cannot be adequately described by an axial dipole term alone, the GAD hypothesis is still used in PSV studies. References to the time-averaged field in the palaeomagnetic literature are often confusing, as the definition of 'time-averaged' is usually not rigorous, and varies from one study to another. In this paper, we use the term 'time-averaged' to mean the average field direction at a particular site over a given time interval, that is

$$\langle \hat{B} \rangle = \int_{t_1}^{t_2} \hat{B}\, \mathrm{d}t/(t_2 - t_1).$$

($\hat{B}$ is the unit vector in the direction of the magnetic field at a given location.) The evaluation of $\langle \hat{B} \rangle$ at a particular site would be quite straightforward if we knew t_1 and t_2, and had a good temporal distribution of data over this time interval. However, as noted at the beginning of this paper, palaeomagnetic studies rely on data which is unevenly distributed in time and space, and so the estimation of $\langle \hat{B} \rangle$ is a statistical problem. We assume that if we can make an estimate of the time interval $t_2 - t_1$ (discussion of this issue below), and if we have a sufficient temporal distribution of data (see criteria (7)–(9) of § 2 *a*) over this time interval, then we can approximate $\langle \hat{B} \rangle$ by the average field direction computed from our finite set of palaeomagnetic directions. Obviously, this assumption can lead to problems if the data do not adequately sample the palaeosecular variation of the field over the time interval used for averaging. Another problem is that this uneven temporal sampling differs from one location to another, and so our estimates of $\langle \hat{B} \rangle$ may be of variable reliability. This issue can be addressed somewhat by careful data selection during the compilation phase, and by careful assignment of uncertainties to the estimated mean directions. We discuss this later in the context of the database presented here.

One problem encountered when we attempt to describe the time-averaged field is that we do not have a good estimate for characteristic timescales of secular variation and, hence, it is not clear over what time period we need to examine the geomagnetic field to obtain a reliable average field model. In other words, we do not know what t_1 and t_2 are in our definition of 'time-averaged'. Ideally, we would like to have a mathematical description for PSV based on physics, this model being supported by the available data. Characteristic timescales of this model would provide a theoretical, rather than empirical basis for establishing time windows over which we could obtain an estimate of the average field configuration, given sufficient high quality data. Unfortunately, to date, only empirical estimates for such characteristic timescales are available, and often these estimates are based on few data. Conservative bounds on PSV timescales can be obtained by looking at individual PSV records; for example, a power spectral analysis (Barton 1983) of observatory, archaeomagnetic and sedimentary PSV data gave a broad peak in the spectrum over periods of 10^3–10^4 years. Although some of the results of this analysis are artefacts due to the wide variety of variable-quality data used, the presence of the broad peak in the spectrum is supported by individual lake-sediment records. For example, lake-sediment records from Australia (Barton & McElhinny 1981) and Great Britain (Thompson & Turner 1979) suggest that periods of at least a few thousand years are necessary to obtain an estimate of the average field at these locations. These results provide some constraints on the minimum period necessary to average out PSV; an upper limit on this time period is suggested by the database presented here. Statistical testing suggests that the Brunhes (0–0.78 Ma) and the remaining normal polarity data (0.78–5.0 Ma) do not exhibit statistically significant different average field properties (for example, the Kolmogorov–Smirnov test (Kendall & Stuart 1979). Details of the application of this test to the new database are presented in another paper, specifically concerning the question of the time-averaged field structure (Johnson & Constable 1995). The important result for our purposes here is that we can place conservative bounds of 1000–780 000 years on the time period which should be sampled to obtain a good estimate of PSV and the time-averaged field.

Figure 1 illustrates at least two of the concerns mentioned above. Both figures 1*a* and *b* show the VGP dispersion for the palaeosecular variation from lavas (PSVL) data used by McFadden *et al.* (1988, 1991) and the best-fit model (model G) to the data with 95% confidence limits. All VGP positions are mapped into the Northern Hemisphere and the dispersion is averaged in latitude bands as described in McFadden *et al.* (1991). The GAD hypothesis was assumed and so VGP dispersion was calculated about the geographic pole. Figure 1*a* also shows the latitudinally averaged VGP dispersion for the new database presented in this paper, where the dispersion is calculated about the geographic pole. In figure 1*b*, the dispersion for the new database is calculated about the mean pole position for each group of data as a crude way of estimating dispersion when the time-averaged field is not the GAD. This figure illustrates the importance of the data coverage in PSV studies and the effect of the time-averaged field we assume in the study.

2. Database

(*a*) *Selection criteria*

The database presented in this paper contains palaeomagnetic directions tabulated in refereed journals and which satisfy the following criteria:

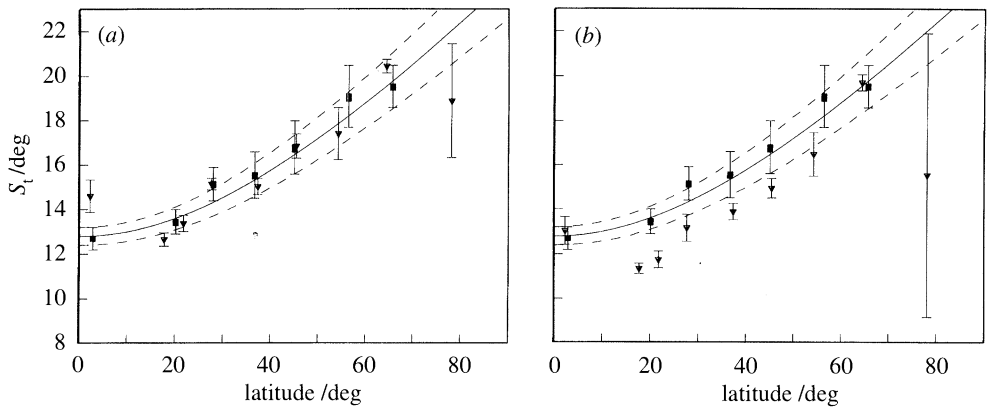

Figure 1. VGP dispersion for the past 5 Ma. Squares (in both (*a*) and (*b*)) represent data of McFadden *et al.* (1988, 1991). Uncertainties are two standard errors in the mean, computed using a jacknife. The solid line represents the best-fit model G of McFadden *et al.* (1991) with the 95% confidence limits to this model as the dashed lines. In (*a*) the triangles represent the VGP dispersion for the revised data set computed about the geocentric axial dipole, in order to compare directly with that of McFadden *et al.* (1991). In (*b*) a different time-averaged field is mimicked by computing the VGP dispersion about the mean pole (triangles) for each group in the revised data set. The VGP scatter for the new data set includes some experimental error which is not taken into account. This small effect has been corrected for by McFadden *et al.* (1991).

(1) only extrusives and thin intrusives (i.e. thin dykes) were used;

(2) the individual magnetically cleaned flow directions must be published;

(3) the reference from which the data are taken was published during the period 1965–1992;

(4) at least three samples per flow were taken in the field;

(5) the VGP latitude corresponding to each field direction must be at least 55° in magnitude;

(6) the estimate of the precision parameter must be greater than 30 for directions to be accepted as significant;

(7) there is sufficient information in the reference to establish temporal independence of the flows;

(8) temporal sampling from a given location must span at least 10 000 years; and

(9) we require at least five flows satisfying criteria (1)–(8) at any given location.

Extrusives and thin intrusives are required to ensure that the thermal remanence was acquired instantly on geological timescales, and the individual magnetically cleaned (to remove overprinting) flow data must be published to obtain an estimate of the statistics of the temporal variation of the field at a given location. Data published before 1965 were not included on the grounds that laboratory methods, specifically the magnetic cleaning of samples, were less advanced and these data may be unreliable.

In any PSV study it is necessary to be able to estimate field and experimental uncertainties, so we require at least three cores per flow to have been taken. Typically 2–8 cores per flow are taken during palaeomagnetic field work. Some studies have attempted to estimate the minimum number of samples required to average out field measurement uncertainties. For example, Ellwood *et al.* (1973) estimated that the largest number of samples per flow required to obtain a reliable mean direction was four. We found that a high percentage of flows where only two samples were taken did

not meet other selection criteria such as the VGP latitude cut-off, and so we decided to exclude all two-samples-per-flow data.

Low VGP latitudes may indicate unusual secular variation, but are also associated with excursions and reversals which are not considered part of the normal secular variation record. PSV studies generally assume a cut-off VGP latitude of 45–60°; we used a value of 55° and flows with field directions corresponding to VGP latitudes less than this value were excluded from the database. Often, one or two low-latitude VGP data are reported from a series of flows which otherwise have palaeodirections associated with high latitude VGPs. These low-latitude VGPs are usually the result of field or laboratory measurement errors, rather than being indicative of either a field excursion or anomalously high secular variation. In such cases, we found that VGP latitude data in the range 45–55° often failed other selection criteria. On the other hand, several low-latitude VGPs from one site may indicate high secular variation or an excursion. We used a VGP cut-off of 55° in order to try to ensure that estimates of secular variation from this database would be conservative rather than anomalously high due to the inclusion of excursion data. Previous secular variation models have suggested that VGP dispersion at high-latitude sites can be as large as 20–25°, thus our choice of a 55° cut-off for VGP latitude is intended to include normal secular variation data from high latitudes.

The Fisherian precision parameter provides information on whether a given set of directions are statistically different from a random population, a precision parameter of zero indicating a completely random population. Thus, for each flow we would expect the set of directional measurements, corresponding to the cores from that flow, to have a high precision parameter, assuming correct orientation of the samples and reliable laboratory techniques. Choosing a cut-off value for the precision parameter is somewhat *ad hoc* – we have used a value of 30, with a few exceptions where many records counteracted the lower quality of some of the contributing data. Obviously, reliable estimates of secular variation require sufficient data spanning the longest timescales of the variation, and criteria (7)–(9) represent an attempt to ensure adequate sampling. Of all the criteria, (7) and (8) are the most difficult to enforce as they are subjective and dependent on age dating of the flows and/or good geological descriptions of the study areas in the original reference.

(*b*) *Data sources*

The data sources used to obtain the references for this compilation were the Lee database (1983), the Global Paleomagnetic Database (GPMDB) (Lock & McElhinny 1991), and additional library search by the authors for post-1988 data. The final data set comprises 2187 records from 104 distinct locations – 1528 normal polarity records and 659 reverse polarity records. Of the 2187 records, only 1272 were taken from the original Lee database, which comprises 2244 records in its original form. The severe editing of the Lee database was largely a result of the presence of many records (323) consisting of fewer than three samples per flow. After consulting the original references, we also decided that in some cases there was insufficient information to determine whether the flows sampled were temporally independent or whether they covered a sufficiently long time span to provide a good estimate of secular variation. A few records in the Lee database had VGPs with latitudes less than 55°, others had values of the precision parameter which we considered unacceptably low, or the precision parameter could not be estimated. 729 records were added from references in the GPMDB, but not in the Lee database. Another 186 records were added which were not referenced in either the Lee database or the GPMDB. Relevant details of

PHILOSOPHICAL TRANSACTIONS OF THE ROYAL SOCIETY A MATHEMATICAL, PHYSICAL & ENGINEERING SCIENCES

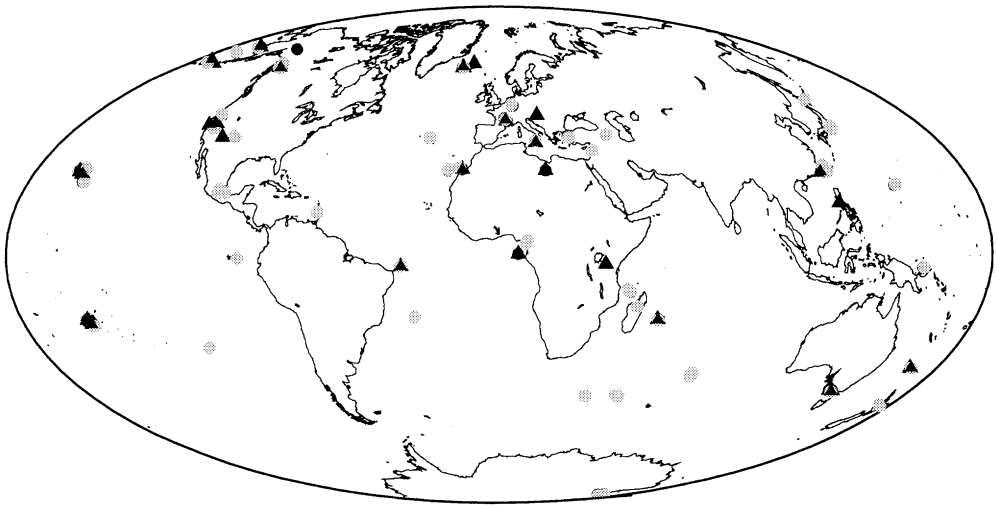

Figure 2. Location map for the data comprising the revised database. The circles denote normal polarity data, the triangles denote reverse polarity data.

the individual studies contributing to the database are given in the appendix. The study locations are shown in figure 2.

(*c*) *Local properties of the database*

Before considering global properties of the palaeofield and PSV we mention some local properties of the field observed in the new database. Mean declinations, inclinations, VGP positions and the associated 95% confidence cones (Fisher 1953) are given in table 1 for the normal and reverse polarity data separately. Note that these VGP positions, with their 95% confidence cones are plotted in the figures in the appendix. First, we observe that all but ten of the data groups have 95% confidence cones of less than 10°, and eight of these ten locations have less than ten flows contributing to the estimate of the mean direction. Based on the selection criteria, we have no reason for excluding these sites with rather poorly constrained mean directions: it is important to note that other sites with less than ten flows do have a well-constrained mean direction. However, these sites are noted here as a reminder that they should be considered carefully in any global analyses. Second, we note that the 95% confidence cones about the mean direction are in most cases much less than our estimates for secular variation (described in the next section). This is important because it implies that our secular-variation estimates should be reasonably robust with respect to the mean direction at a given location. Third, we can see from table 1 that there are some large differences (10–15°) in the mean directions calculated for neighbouring sites. In most of these cases, the 95% confidence cones about the mean directions intersect. In a few cases, neighbouring mean directions do appear to be significantly different and this may indicate that the palaeomagnetic sampling at one or both sites is insufficient (in a temporal sense) to obtain a reliable estimate of PSV and the mean field direction at that location. Again, these cases should be treated with care in global analyses.

(*d*) *Availability*

The database itself is available on-line, subdivided according to geographical region and normal or reverse polarity. A '`README`' file provides file format details. The data can be obtained from the authors by anonymous ftp as follows.

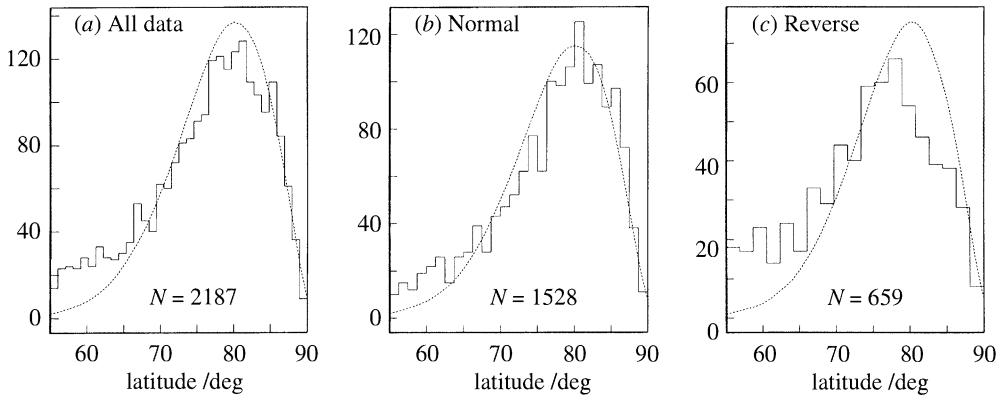

Figure 3. VGP latitude histograms for the revised database (solid lines) compared with the smoothed predictions of the Constable & Parker (1988) secular variation model (dashed curves), calculated at the site locations. N is the number of data in each histogram; (a) shows all the 0–5 Ma data, (b) shows normal polarity data only, and (c) shows reverse data.

```
% ftp 132.239.154.16  or  ftp ozzy.ucsd.edu
% login: anonymous
% password: username@usermachine
> cd pub/pmag5
> mget *
> quit
```

3. Palaeosecular variation

Previous PSV models, and the data used in these models, were discussed in the introduction. Several concerns were raised which fall into four main categories: data distribution, quality control of data, the structure of the time-averaged field and problems associated with using VGP positions. In this section we review various statistical properties of the revised database, especially those which highlight one or more of the four major concerns outlined above. We compare properties of the database with the Constable & Parker (1988) model as it is the most recent global PSV model and is constructed in a manner which allows us to distinguish between the effect of long-period bias and temporal variability in the data. This section presents some global properties of the database, as opposed to local features described in the previous section.

(a) *Data distributions*

VGP latitude and longitude distributions for the revised data set are given in figures 3 and 4 together with the smoothed predictions of the Constable & Parker (1988) model at the database site locations. Reverse polarity VGP positions are mapped into the antipodal pole position.

The Constable & Parker (1988) model fits the general shape of the combined polarity VGP latitude distribution (figure 3), with the exception of the low latitude VGP data. The fit of the model to the normal polarity data alone is similar, but the model does not predict even the general shape of the reverse polarity data distribution: the mode for the model is about 5° greater than for the data, the variance in the model distribution is too low and the low-latitude VGPs in the data distribution

Table 1. *Mean directions and mean VGP positions for each data group with 95% confidence cone*

(λ_s site latitude; ϕ_s site longitude; N, number of flows; n, mean number of samples per flow; I, mean inclination; D, mean declination; α_d, 95% confidence cone for mean direction, λ_v, mean VGP latitude; ϕ_v, mean VGP longitude; α_v, 95% confidence cone for VGP.)

λ_s	ϕ_s	N	n	I	D	α_d	λ_v	ϕ_v	α_v
				Normal polarity					
−78.39	164.23	13	7	−83.85	−59.10	3.733	78.41	46.36	7.042
−78.39	164.23	13	7	−83.85	−59.10	3.733	78.41	46.36	7.042
−77.56	166.26	5	8	−87.32	6.90	7.759	83.02	−16.34	14.777
−46.90	37.80	15	7	−67.30	7.89	5.500	83.00	173.21	7.952
−46.50	51.70	32	4	−64.50	−2.66	3.230	88.46	−66.70	4.476
−46.50	52.20	37	4	−60.52	10.14	3.480	82.17	115.37	4.751
−38.80	77.50	14	7	−58.14	−10.81	8.039	81.91	−27.75	10.101
−38.50	175.00	19	8	−60.73	0.53	3.470	86.15	−6.33	4.738
−38.00	142.80	5	3	−55.03	−1.33	9.243	87.34	116.01	12.954
−38.00	144.50	17	3	−61.14	5.90	2.933	83.56	−80.33	4.351
−37.83	77.52	24	7	−59.25	5.33	4.275	84.61	−152.33	5.116
−29.10	167.90	25	3	−42.14	11.42	2.840	78.86	−122.98	2.769
−27.10	−109.20	53	3	−45.00	1.05	3.125	89.58	−17.09	3.551
−21.10	55.50	17	7	−38.94	−1.17	6.800	87.94	−90.72	6.657
−21.00	55.50	27	5	−47.20	−4.28	3.610	80.97	−98.11	3.841
−20.52	−29.33	5	3	−40.99	−0.44	3.781	86.97	158.54	4.216
−17.67	−149.58	23	5	−29.09	3.92	4.525	85.86	−81.95	3.399
−17.67	−149.58	8	4	−31.03	−2.65	7.509	87.37	133.00	6.522
−17.00	47.50	14	5	−43.63	−10.20	7.150	77.14	−92.11	7.330
−16.83	−151.45	8	4	−30.87	4.45	7.444	85.75	−59.99	6.644
−16.75	−151.00	32	4	−31.93	−0.07	4.078	89.01	20.91	3.864
−16.50	−151.27	7	3	−34.03	5.64	6.120	84.05	−37.56	5.802
−12.20	44.40	23	5	−22.09	2.81	5.402	87.53	126.58	4.539
−11.60	43.30	12	5	−20.16	−2.97	5.032	86.85	−27.65	4.053
−4.00	150.00	5	3	−14.95	−2.39	15.626	85.52	2.55	14.138
−3.85	−32.40	7	8	−8.56	−9.68	3.084	80.34	−125.47	2.498
−0.83	−88.42	18	8	2.91	−1.00	5.661	87.49	−113.07	4.366
0.00	6.50	14	3	−5.37	3.94	8.789	80.87	−115.91	8.021
0.00	6.50	9	3	−8.91	−7.33	10.848	85.13	137.66	6.555
3.50	9.00	38	3	−2.31	−0.35	4.830	85.20	−166.80	3.638
4.50	9.50	15	3	5.18	−0.58	7.211	88.12	−151.63	5.024
13.30	−61.20	9	4	18.10	−9.14	8.341	80.37	−172.48	5.742
18.10	145.70	23	6	32.16	1.97	2.780	88.11	−110.13	2.284
19.00	−99.00	30	6	29.43	1.31	4.090	86.94	62.99	3.617
19.20	−98.60	21	7	34.17	3.73	6.257	85.78	−18.15	5.201
19.30	−96.90	20	9	30.83	−0.73	5.296	87.83	97.78	4.601
19.40	−155.50	7	7	31.45	10.19	14.044	79.71	−60.39	10.598
19.50	−155.50	25	6	25.05	0.47	5.337	78.62	−22.14	4.289
19.50	−155.50	28	5	21.66	8.38	4.919	82.77	−51.01	2.736

Table 1. *Cont.*

λ_s	ϕ_s	N	n	I	D	α_d	λ_v	ϕ_v	α_v
19.50	−155.50	29	5	31.72	7.50	3.393	84.28	21.94	3.703
19.60	−99.00	23	6	33.94	1.95	6.169	87.42	−10.05	5.426
21.30	−157.80	25	7	32.10	−0.08	3.810	86.42	20.77	3.233
21.50	−158.10	31	7	33.98	−0.43	4.458	87.69	37.16	4.022
22.00	−159.50	46	4	27.45	−3.57	4.253	82.62	48.44	3.287
22.00	−160.00	11	6	26.79	−7.23	5.308	79.79	63.19	4.509
23.10	−158.00	14	7	35.62	2.70	7.960	86.82	−26.56	6.094
23.50	121.40	12	4	31.99	3.86	8.228	83.98	−96.66	7.462
25.30	121.50	27	5	38.50	1.27	5.159	87.05	−76.77	4.562
27.80	−18.00	10	4	45.62	6.72	10.034	84.66	66.36	9.469
27.80	17.30	10	3	34.09	5.07	5.336	80.16	168.70	4.203
28.20	−12.80	18	4	40.55	−2.05	5.633	85.08	−169.16	5.873
28.70	−14.20	14	5	41.94	3.27	6.843	85.14	129.23	7.486
34.00	36.00	9	5	49.09	−3.66	7.151	85.86	−105.59	7.936
35.00	139.00	13	7	53.71	−5.52	3.979	85.40	48.89	4.726
35.21	138.77	35	4	49.82	−4.99	3.893	84.75	6.46	4.359
35.90	−106.50	6	7	43.88	−1.77	3.267	79.74	82.85	3.314
35.90	−106.50	6	8	51.44	0.38	5.844	86.66	65.09	5.909
37.67	−119.00	33	7	55.80	−0.59	4.125	89.68	141.40	4.860
38.00	15.00	14	14	56.26	−1.74	3.888	88.31	−107.87	5.135
38.60	28.70	5	8	61.60	11.60	3.929	80.32	87.91	4.876
38.70	−27.20	20	7	52.48	−2.83	5.969	84.92	−177.57	6.558
39.50	44.00	5	6	51.33	3.44	10.301	83.04	−155.36	10.822
41.75	−121.85	16	6	50.82	4.50	4.719	79.97	36.12	5.251
43.50	143.50	13	17	57.45	−13.48	5.257	78.60	31.84	7.234
44.69	4.30	5	7	51.51	−10.52	10.961	74.87	−136.05	13.915
45.00	3.80	7	3	61.56	8.18	7.543	83.10	102.18	10.266
45.71	2.99	26	6	61.90	−0.18	3.597	88.38	−168.61	4.802
50.30	6.75	37	14	67.97	10.03	3.275	83.39	78.85	5.050
50.40	7.25	30	13	67.17	3.06	3.009	87.78	87.21	4.361
53.00	−172.00	53	6	69.35	0.07	1.879	89.25	−150.38	2.882
57.18	−170.36	8	6	63.31	3.82	7.810	78.77	0.80	11.424
57.50	−130.00	16	3	75.00	−6.21	5.370	83.74	−162.93	9.103
58.50	−131.50	11	4	69.82	13.48	6.652	82.08	−21.95	9.989
59.99	−165.87	13	7	73.20	1.69	4.920	89.01	−48.33	8.287
60.33	−166.09	8	7	78.46	18.09	4.858	79.09	−128.28	8.964
62.92	−143.16	9	4	75.97	−6.99	3.702	86.45	147.57	5.942
64.50	−21.50	29	3	73.61	−7.37	4.444	82.44	139.00	4.518
64.50	−21.50	52	3	71.44	4.44	2.871	85.26	−153.82	7.176
64.50	−22.00	10	3	71.73	26.56	5.488	74.80	85.46	9.197
64.50	−22.00	65	3	75.87	5.64	2.223	87.23	77.37	3.831

PHILOSOPHICAL TRANSACTIONS OF THE ROYAL SOCIETY A MATHEMATICAL, PHYSICAL & ENGINEERING SCIENCES

Table 1. *Cont.*

Reverse polarity									
−38.00	142.80	5	3	59.11	−165.20	11.584	−77.28	74.68	12.937
−38.00	144.50	14	3	57.81	−179.38	3.614	−88.71	106.92	4.262
−29.10	167.90	12	3	38.62	−164.08	3.576	−74.07	54.77	3.294
−21.00	55.50	13	3	45.84	178.81	6.868	−82.78	66.03	7.159
−17.67	−149.58	39	6	32.36	179.31	3.947	−88.86	−93.41	3.103
−17.53	−149.85	6	3	34.94	−175.58	9.155	−85.43	152.35	7.332
−16.50	−151.27	6	4	32.99	178.18	9.415	−87.46	−108.02	8.587
−3.85	−32.40	5	4	26.93	171.44	2.218	−76.60	6.03	1.704
−3.20	35.50	12	5	−5.22	179.97	13.672	−83.88	−143.58	9.467
0.00	6.50	14	3	14.29	172.11	8.858	−79.09	52.78	7.388
4.45	120.58	5	7	−17.40	172.85	7.888	−81.21	173.35	5.317
21.50	−158.10	27	7	−24.31	177.44	5.969	−81.68	−141.70	4.574
21.50	−158.10	33	7	−29.83	178.86	4.429	−85.02	−141.91	3.435
22.00	−159.50	42	6	−29.87	−176.73	2.198	−83.34	171.62	2.107
22.00	−160.00	5	7	−38.26	−171.03	6.132	−81.79	110.04	4.944
23.60	119.50	7	8	−28.67	−179.80	10.054	−82.41	118.99	7.242
27.80	17.30	54	3	−47.09	−170.71	3.302	−81.06	−84.95	3.101
28.20	−12.80	6	4	−38.94	178.04	10.790	−84.55	0.84	10.370
35.50	−111.60	9	8	−51.87	173.52	7.290	−84.50	−43.15	9.164
37.20	14.80	6	10	−54.03	178.61	4.948	−87.61	40.89	5.330
38.50	−122.50	13	8	−42.78	−178.36	6.469	−76.61	−129.50	7.133
39.25	−120.00	6	5	−54.91	170.76	9.094	−81.98	−50.31	11.499
45.00	3.80	13	3	−56.47	−169.12	5.720	−78.89	−52.321	6.745
46.90	17.50	6	7	−65.17	168.67	8.394	−82.12	124.59	11.434
53.50	−168.10	8	5	−71.92	−171.47	9.571	−82.47	56.16	15.03
57.50	−130.00	44	4	−68.96	−168.66	3.007	−82.30	165.88	4.616
60.33	−166.09	8	7	−74.95	−171.61	8.324	−85.06	56.11	12.643
64.50	−21.50	12	3	−78.19	−169.984	6.320	−77.02	−8.38	14.210
64.50	−21.50	68	3	−75.78	−179.24	2.656	−83.85	−154.88	10.874
64.50	−21.50	8	3	−67.91	175.89	9.200	−89.68	−76.92	4.459
64.50	−22.00	103	3	−74.66	179.48	2.193	−78.90	−56.13	8.963
64.50	−22.00	15	3	−69.70	−170.44	5.772	−82.31	−49.44	7.809
64.50	−22.00	16	3	−71.51	−174.78	5.042	−88.23	−37.60	3.517
66.20	−15.20	19	4	−74.29	−174.70	4.802	−85.23	−44.90	7.762

are not modelled. The main signal common to all the VGP latitude distributions is the location of the mode at around 80° latitude. As discussed earlier, several previous studies have suggested that the time-averaged geomagnetic field has a non-zero mean axial quadrupole component, causing a 'far-sided' effect in VGP locations (the VGP plots on the other side of the geographic pole from the site location). Obviously, VGP latitude distributions alone cannot distinguish between a 'far-sided' and

PHILOSOPHICAL TRANSACTIONS OF THE ROYAL SOCIETY A MATHEMATICAL, PHYSICAL & ENGINEERING SCIENCES

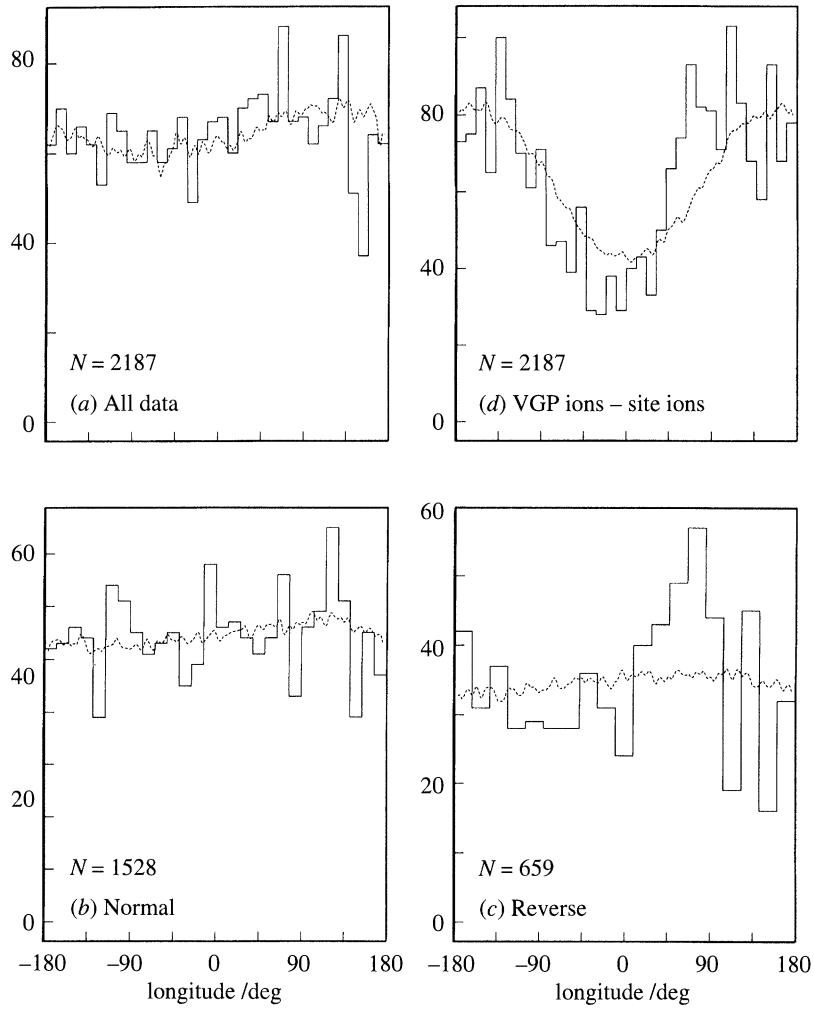

Figure 4. As in figure 3 but for the VGP longitude distributions. Also shown is the distribution of VGP longitudes minus site longitudes ('common-site longitude' plot (*d*)), together with the predictions of the Constable & Parker (1988) model.

a 'near-sided' effect; however, the distributions in figure 3, coupled with figure 4 and the VGP stereo plots shown in the appendix, do indicate that the strongest signal in the time-averaged field is the 'far-sided' effect. Figure 3 also suggests that there may be differences between the average field during normal and reverse polarities. Such a difference has been suggested by other workers, using other datasets; for example, Schneider & Kent (1990) proposed different average field configurations for normal and reverse fields based only on inclination data from deep-sea cores. Direct comparisons between such studies are difficult since different datasets have different abilities to resolve temporal and spatial structure in the field.

Differences between the normal- and reverse-polarity data are also seen in the VGP longitude distributions (figure 4). The combined polarity distribution shows peaks at longitudes of 70° and 125° and a trough at 150° but is otherwise fairly homogeneous with longitude. The peak at 70° is due to both reverse and normal polarity data, that at 125° is due primarily to the normal polarity data. It is evident that

the Constable & Parker model (1988) predicts the general shape of the longitude distributions, but is unable to predict the amplitude of the distribution peaks. We attribute part of this discrepancy in the VGP longitude distributions to having insufficient data from a statistical sampling standpoint. The VGP latitude distributions (figure 3) are mapped onto a 35° interval, whereas the VGP longitude distributions (figure 4) span 360°. This effect is particularly noticeable in the model predictions. The model distributions for VGP latitudes are much smoother than those for the VGP longitudes, indicating that the current data distribution is still not ideal for investigating longitudinal spatial field variations. The general homogeneity seen, in the VGP longitude distribution for combined normal- and reverse-polarity data, is in general agreement with that obtained by Quidelleur *et al.* (1994) in an independent revision of the Lee database, although their final database differs from that presented here because of the different selection criteria used. The distribution of VGP longitudes for both this new revised database and that of Quidelleur *et al.* is significantly different from that reported by Constable (1992). Implications of this are discussed briefly in the summary section of this paper and in a separate paper concerning the structure of the time-averaged field (Johnson & Constable 1995). For now, it suffices to say that the difference between the VGP longitudes obtained from this database and those reported by Constable (1992), plus the statistical sampling considerations mentioned, emphasize the importance of a reasonable data distribution and the importance of consistent quality control on data to be used for PSV studies.

Figure 4 also shows VGP longitudes for combined normal and reverse polarities, plotted relative to their site longitudes. This type of plot is often referred to as a 'common-site longitude' plot and is a crude attempt to remove the effect of uneven sampling. The predominant feature of this plot in figure 4 is that VGP longitudes generally lie at least 90° away from the site longitude. VGP positions having a latitude less than 90° and a VGP longitude 180° away from the site longitude are pure 'far-sided' VGPs. The database presented here demonstrates this 'far-sided' effect, although the strength of the signal appears to vary on a regional basis (see appendix), and there are more near-sided VGPs than predicted by the Constable & Parker (1988) model.

Egbert (1992) showed that the VGP longitude distribution is related solely to the secular variation for the non-axial dipole part of the field and that there is a tendency for VGP longitudes to be biased 90° away from the sampling site for rotationally symmetric (homogeneous or isotropic) field models. The magnitude of this bias depends upon the field model, specifically upon the ratio of the variance in the vertical field to the variance in the horizontal field. This ratio is referred to as κ^2. For homogeneous field models, this parameter falls in the range $2 < \kappa^2 \leqslant 4$, where κ^2 is equal to 4 for a purely dipolar model and tends to 2 for fields dominated by short-wavelength features. The Constable & Parker (1988) model has a value for κ^2 of 3.2. The tendency of VGP longitudes to be 90° away from the site longitudes is least (flat VGP longitude distribution) for $\kappa^2 = 4$ and increases as κ^2 decreases. Important in palaeomagnetic work is the effect of measurement uncertainty on the study in hand. Measurement error can be modelled as isotropic noise where the vertical and horizontal variances in the field are equal, i.e. $\kappa^2 = 1$. This produces the greatest bias in VGP longitude distributions. Figure 5 shows the results of these different models, where the model VGP longitude distributions are calculated for the site distribution in the new database. We can see qualitatively that the incorporation of isotropic measurement noise ($\kappa^2 = 1$) into a given field model could produce substantial variations in the VGP longitude distributions. The presence of such isotropic noise could be one reason why

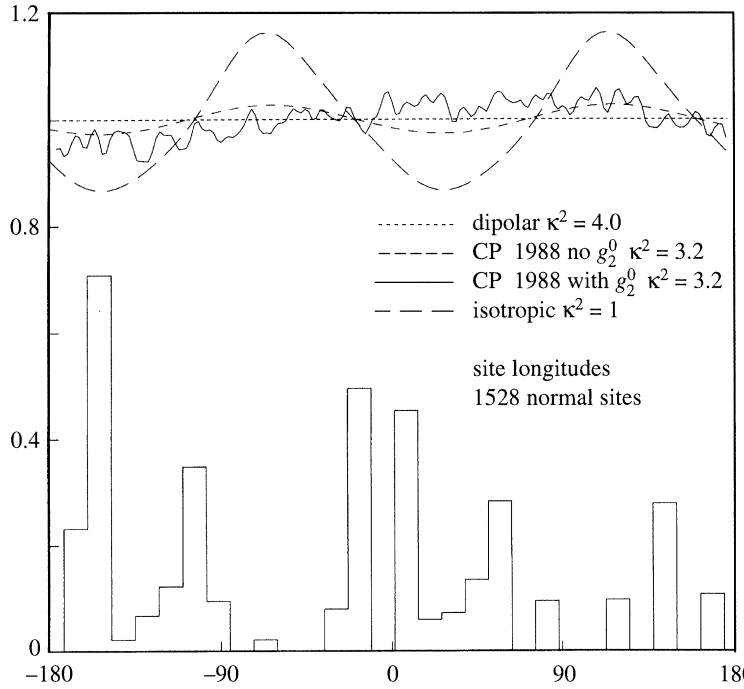

Figure 5. VGP longitude distributions for four PSV models at 0–5 Ma sites ($\kappa = \sigma_z/\sigma_x$). The data-site longitude distribution is shown in the lower part of the figure. The smoothed predictions of the Constable & Parker (1988) model, both with and without a zero mean axial quadrupole, are shown. The uniform distribution is for a purely dipolar field and the long dashed line shows the predictions of an isotropic secular variation model in which the vertical and horizontal variances are equal (Egbert 1992).

the common-site longitude plot in figure 4 does not exhibit a pure 'far-sided' effect. The difference between the distributions predicted by the Constable & Parker model (1988) for two time-averaged field structures (with and without an axial quadrupole term) demonstrates that knowledge of the time-averaged field structure and reliability of the palaeomagnetic measurements are critical in PSV studies. We note here that nonlinear least-squares fits for a time-averaged field structure (up to spherical harmonic degree 10), to the palaeodirections presented in this paper, yield spatially complex field models. In such models, the magnitudes of some of the higher-degree and higher-order spherical harmonic coefficients are comparable to the magnitudes of low-degree coefficients, such as the axial quadrupole and octopule terms. In contrast, inversions for a spatially smooth time-averaged field model suggest that the predominant non-axial-dipole signal in the current database is the axial quadrupole term, although there is still evidence for other non-dipole terms (Gubbins & Kelly 1993; Johnson & Constable 1995).

(*b*) *Calculation of dispersion*

Traditionally, the measure of secular variation which has been modelled is the angular dispersion in either the field directions or the VGP positions. First, it is necessary to define some terminology. Suppose we sample a series of N temporally independent lava flows at a given location. From each flow, we take n_i palaeomagnetic samples and calculate a mean field direction for that flow. We thus have N pairs of measurements of declination D and inclination I at a given location. We can now

investigate the secular variation record retained by this series of flows as follows. The total angular variance (dispersion) in the field directions and VGPs, respectively, are given by

$$s_t^2 = \frac{1}{N-1}\sum_{i=1}^{N}\delta_i^2, \tag{3.1}$$

$$S_t^2 = \frac{1}{N-1}\sum_{i=1}^{N}\Delta_i^2, \tag{3.2}$$

δ_i is the angle between the direction vector from the ith flow and the time-averaged mean direction vector at our study location. Δ_i is the corresponding angle between the ith VGP position and the time-averaged mean pole. Immediately apparent is the necessity for a time-averaged field model before secular variation can be modelled. As explained in the introduction, PSV studies have generally assumed that the GAD describes the time-averaged field. Hence, the mean VGP position to be used in calculating Δ_i in (3.2) conveniently corresponds to the geographic north pole. The mean field direction to be used in calculating δ_i in (3.1) is the field direction at the ith location which would be produced by a GAD field.

The dispersion obtained by calculating (3.1) or (3.2) cannot be compared directly with that predicted by secular variation models. The total field dispersion is made up of two components, the within-site dispersion (due to experimental uncertainty) and the true-field dispersion known as the between-site dispersion. Thus, (3.1) and (3.2) can also be written as

$$s_t^2 = s_b^2 + s_w^2/n, \tag{3.3}$$

$$S_t^2 = S_b^2 + S_w^2/n, \tag{3.4}$$

where n is the average number of samples per site (flow) and s_w^2 and S_w^2 are, respectively, the average within-site dispersion in field directions and VGPs at this location, that is

$$n = \frac{1}{N}\sum_{i=1}^{N} n_i, \tag{3.5}$$

$$s_w^2 = \frac{1}{N}\sum_{i=1}^{N} s_{w_i}^2, \tag{3.6}$$

$$S_w^2 = \frac{1}{N}\sum_{i=1}^{N} S_{w_i}^2, \tag{3.7}$$

The within-site dispersion can be estimated using Fisher statistics, where the Fisher distribution is the spherical analogue of the Gaussian distribution (Fisher 1953). This is justifiable in that it is reasonable to assume some isotropy in the distribution of measurement error. We quote the result without proof (Cox 1970): for the directional data the within-site dispersion for the ith flow can be calculated using

$$s_{w_i}{}^2 = 6561/k_i, \tag{3.8}$$

where the best estimate of k_i (the precision parameter) is

$$k_i = \frac{n_i - 1}{n_i - R_i}. \tag{3.9}$$

R_i is the magnitude of the vector resultant of the n_i individual sample direction vectors from the ith lava flow. Hence, the average within-site dispersion in the directions can be calculated and the true field dispersion at the particular study location obtained. In theory, the same approach can be used to obtain S_{w_i} and, hence, S_w (average within-site scatter) for VGP positions; however, in practice, this is not usually possible as the VGP equivalent of R_i is not recorded in most published palaeomagnetic studies. Sometimes an average value for S_w is recorded: typically the value is in the range 7–13° (McElhinny & Merrill 1975). Where there is no recorded value, investigators sometimes estimate a rough figure. Cox (1970) derived expressions which could be used to transform dispersion in directions into dispersion in VGPs, with either the directional data or VGPs assumed to be samples from a Fisherian distribution. This transformation approach is sometimes used to obtain an estimate of the VGP within-site dispersion from the within-site dispersion in the directions. This is not entirely satisfactory as the expressions of Cox (1970) require the Fisherian distribution to have a very small variance – a criterion which is not always met. Fortunately, in most studies for which a reasonable estimate of the within-site variance in the VGPs is available, the difference between the total scatter S_t and the between-site scatter S_b is small (usually less than about 1°). As a result of this and in order to minimize the number of assumptions made, we use the total scatter S_t when discussing VGP dispersion. For the directional data, we have direct estimates of both s_w and s_t and so we can calculate s_b. This discussion illustrates one advantage of using directional data rather than VGP positions to model secular variation.

So far we have considered the secular variation record at only one location. For comparison with previous studies, we plot dispersion (in the directions and the VGPs) as a function of latitude. Dispersion values are averaged in latitude bands. Suppose there are N_λ study locations in a given latitude band. The band-averaged dispersion is calculated as a weighted mean dispersion from the N_λ locations, where the weights are the number of flows at each location (McFadden *et al.* 1991). The average dispersion is plotted at the weighted mean latitude for that band.

(*c*) *Dispersion results*

Figures 6 and 7 show the raw dispersion results for directional data and VGP positions, respectively, i.e. the dispersion calculated for each data group in table 1. The corresponding band-averaged dispersion results are shown in figures 8 and 9, where the mean dispersion for each latitude band is plotted at the mean latitude. It should be remembered that the true scatter in the field s_b is plotted for the directional data, whereas the total scatter S_t is plotted for the VGP positions. The results for the revised dataset are compared with predictions made from the Constable & Parker (1988) model.

The raw dispersion in the directions for the data (figure 6*b*) shows considerable scatter. A general trend of decreasing dispersion with increasing latitude is evident, although the raw data indicate that this trend is poorly constrained at both high and low latitudes. The lack of data at high southern latitudes, with the exception of two points from Antarctica, means that secular variation in the Southern Hemisphere is only reasonably constrained as far as about 50° S. The northernmost latitude data are from Iceland (figure 2) and the large quantity of data of varying age from this location (see the appendix) provides a good estimate of secular variation. The low-latitude Southern-Hemisphere data shows considerable scatter in the estimates of dispersion. Asymmetry between the Northern and Southern Hemispheres can be seen in both the dispersion in the data and the dispersion predicted at the site

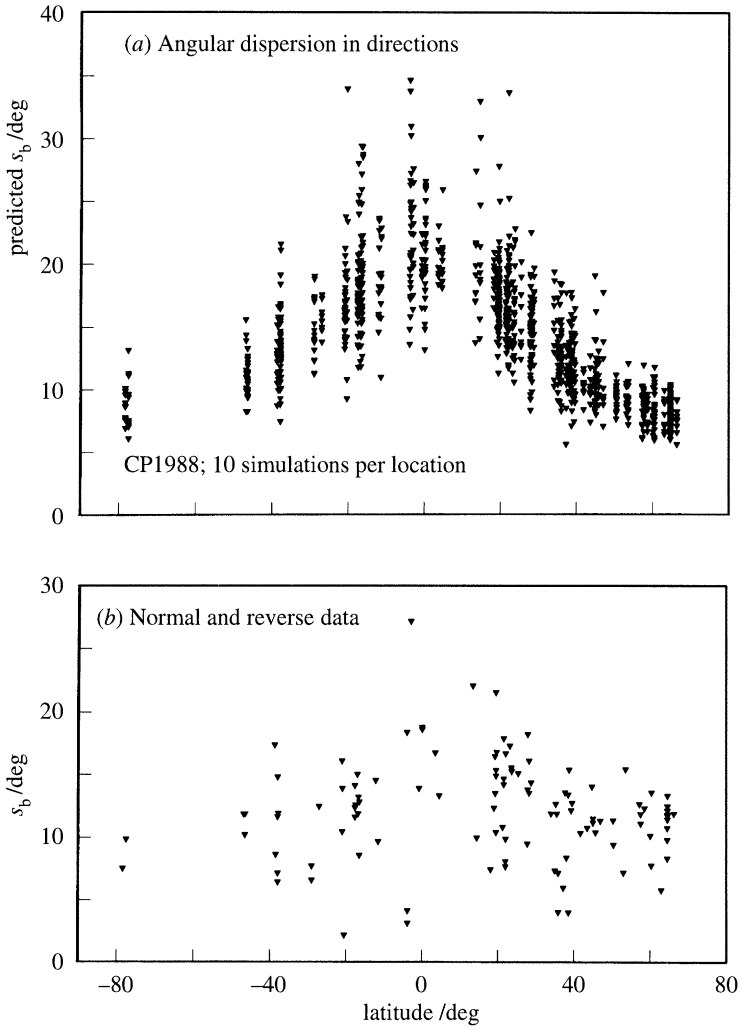

Figure 6. Angular dispersion in directions, computed about the mean direction. (*a*) The predictions of the Constable & Parker (1988) model, where ten simulations are made at each site in the database, to obtain an estimate of the variability expected in the dispersion. For each simulation, the dispersion is computed from N VGP positions, where N is the number of lava flows at that location in the database. (*b*) The results for the combined normal and reverse polarity data. The true scatter in the field s_b is plotted, as the within-site dispersion can be estimated and removed from the total dispersion.

locations by the Constable & Parker (1988) model. Dispersion results for the normal polarity data alone are very similar to the combined polarity results; those for the reverse polarity show the same general trend, although the data distribution for the reverse data is more restricted. At this stage it would be premature to discuss the details of differences in PSV recorded by normal- and reverse-polarity data due to the fact that there are roughly twice as many normal data as reverse, and the fact that the time-averaged field may be different for the two polarities.

In contrast to the behaviour of the direction data, the dispersion in the VGPs predicted by the Constable & Parker (1988) model is almost uniform with latitude (figure 7*a*). This is purely a result of the VGP transformation, but is important as it

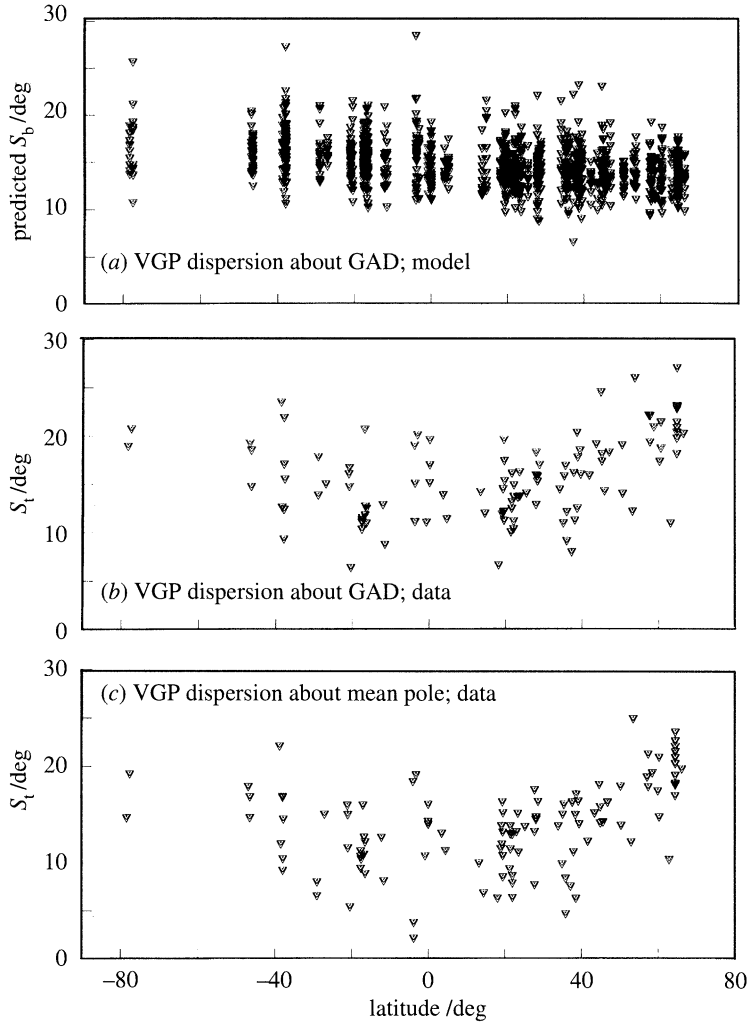

Figure 7. Angular dispersion in VGPs. The model predictions (a) calculated as in figure 6. The data dispersion computed about (b) the geocentric axial dipole and about (c) the mean pole for each group of data, for normal and reverse polarity data combined. The total dispersion S_t is plotted for the data, rather than the between-site dispersion as in figure 6.

demonstrates that any small latitudinal signal in the VGP dispersion may be masked by noise. The VGP dispersion calculated from the data shows a trend of increasing dispersion with increasing latitude, the signal being stronger in the Northern Hemisphere than in the Southern Hemisphere. If real, this trend demonstrates that the Constable & Parker (1988) model is inadequate. The dispersion in the data is calculated about both the axial dipole and the mean pole (where the mean pole is calculated separately for each group of data). Using the mean pole obviously produces a lower value for the dispersion at each location than using the axial dipole, and provides a minimum estimate of the total dispersion for each group of data. As we have not taken into account within-site dispersion in calculating VGP scatter, our S_t values will be slight overestimates of the true VGP dispersion. Some asymmetry in the VGP scatter between the two hemispheres can be seen.

The dispersions averaged in latitude bands illustrate the Northern–Southern-

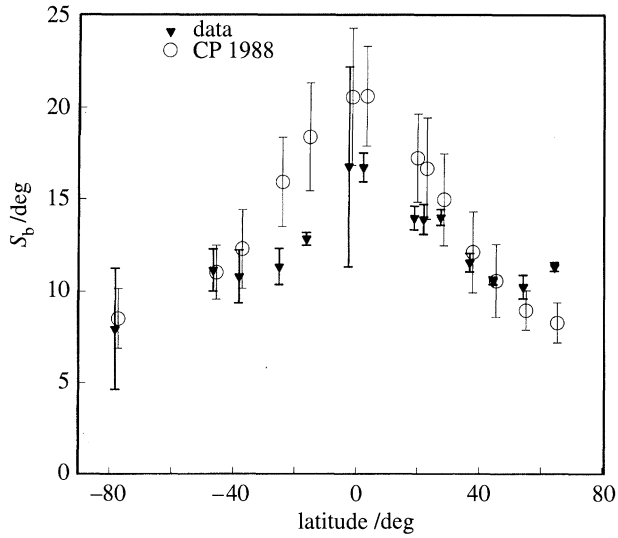

Figure 8. Angular dispersion about the mean direction, averaged in latitude bands. The weighted mean dispersion is plotted at the mean latitude for each band. 100 simulations at each location are computed to obtain a reliable estimate of the mean. Triangles are the data, open circles are the model predictions. The model predictions are offset from the data by 1 deg of latitude for clarity. Uncertainties for the data are two standard errors, computed with a jacknife. Uncertainties for the model are one standard deviation.

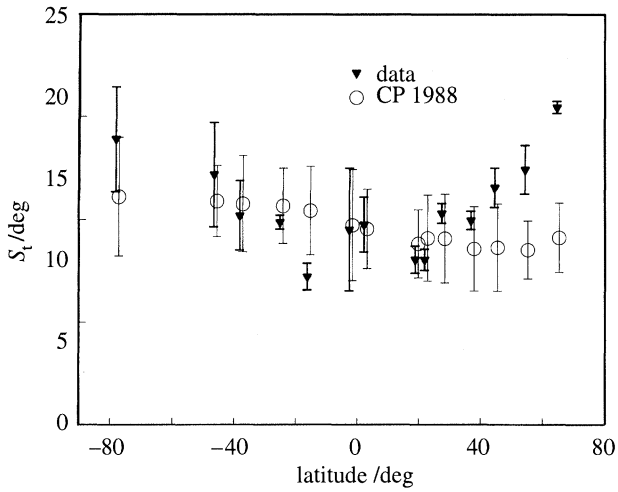

Figure 9. As in figure 8 but for VGP dispersion. The dispersion is computed about the geocentric axial dipole, rather than the mean pole.

Hemisphere asymmetry more clearly, for both the directions (figure 8) and the VGPs (figure 9). The latitudinal variation in dispersion is greater for the direction data than for the VGPs: this observation coupled with the problems in accounting for within-site scatter in estimating VGP dispersion strongly implies that it is advisable to model dispersion in field directions rather than VGP dispersion. Neither the dispersion in the directions nor in the VGPs is modelled very well by the Constable & Parker (1988) model, although the fit to the directional data appears to be slightly better than to the VGPs.

Earlier we noted that the addition of an isotropic noise component (for example, uncertainties in the orientation of samples) to a particular field model could produce substantial variations in the expected VGP longitude distributions for a given data distribution. We have investigated the effect of incorporating orientation uncertainty into the Constable & Parker (1988) model, on both the VGP longitude distributions and the predicted latitudinal variation in dispersion. As before, the predicted dispersion is calculated at each location in the database from N simulations of VGP positions, where N represents the number of lava flows at that location in the database. In the previous dispersion calculations, this procedure is repeated several times (10 times in the case of figures 6 and 7, and 100 times in the case of figures 8 and 9) at each location to obtain an estimate of the variability in dispersion expected from the Constable & Parker (1988) model. To incorporate the effect of orientation uncertainty into the statistical model, each statistical sample from the Constable & Parker model (1988) is taken to define the mean direction of a Fisherian distribution with a given precision parameter. This Fisherian distribution is then sampled once and this new sample replaces the original Constable & Parker model (1988) sample. It is found that this representation of orientation uncertainty produces an improved fit to the VGP longitude distributions and an improved fit to the latitudinal variation seen in the data dispersion curves; however, the total magnitude of the dispersion is too great. The variance in the Constable & Parker (1988) model is then reduced to combat this. Figure 10 shows the results for one such modified model. In this figure, the Constable & Parker (1988) model has been modified so that the total power in the secular variation has been reduced to approximately 40% of its original value. The standard deviation in the horizontal field components is 3.51 μT compared with 5.4 μT in the original model, and the standard deviation in the vertical component is 6.24 μT compared with 9.6 μT originally. At each location, the orientation uncertainty is modelled by sampling from a Fisherian distribution with a mean direction predicted by the Constable & Parker (1988) model and a precision parameter of 100, corresponding to an angular standard deviation of 8.1°. Although we do not wish to attach particular significance to the particular model shown in figure 10, it can be seen that reducing the contribution of the Constable & Parker (1988) model to variance in the field, and incorporating a locally isotropic noise component provides a much better fit to the data. A possible explanation for this could be that orientation errors need to be better accounted for in PSV studies. However, the angular standard deviation of 8.1° for the locally isotropic distribution seems too large to be entirely due to this experimental uncertainty. The local isotropic contribution cannot be modelled by a homogeneous statistical model for spherical harmonics of the kind described by Constable & Parker (1988) (i.e. one in which the secular variation has no preferred coordinate system for the spherical harmonics). An alternative explanation to that of large orientation errors is that the secular variation is inhomogeneous and influenced by a particularly oriented coordinate system (the spin axis or the shape of the CMB). However, before such an issue can be properly addressed, we need a better model for the average field configuration. One final point to note is that while investigating the effect of adding isotropic noise to the statistical model, we noticed that there was often an obvious difference in the goodness of fit of a particular model to the dispersion in the directions or in the VGPs. This is important because it suggests that the 'shape' of the Constable & Parker (1988) model may not adequately describe PSV, as the fit to the data is not robust with respect to the VGP transformation.

PHILOSOPHICAL TRANSACTIONS OF THE ROYAL SOCIETY A MATHEMATICAL, PHYSICAL & ENGINEERING SCIENCES

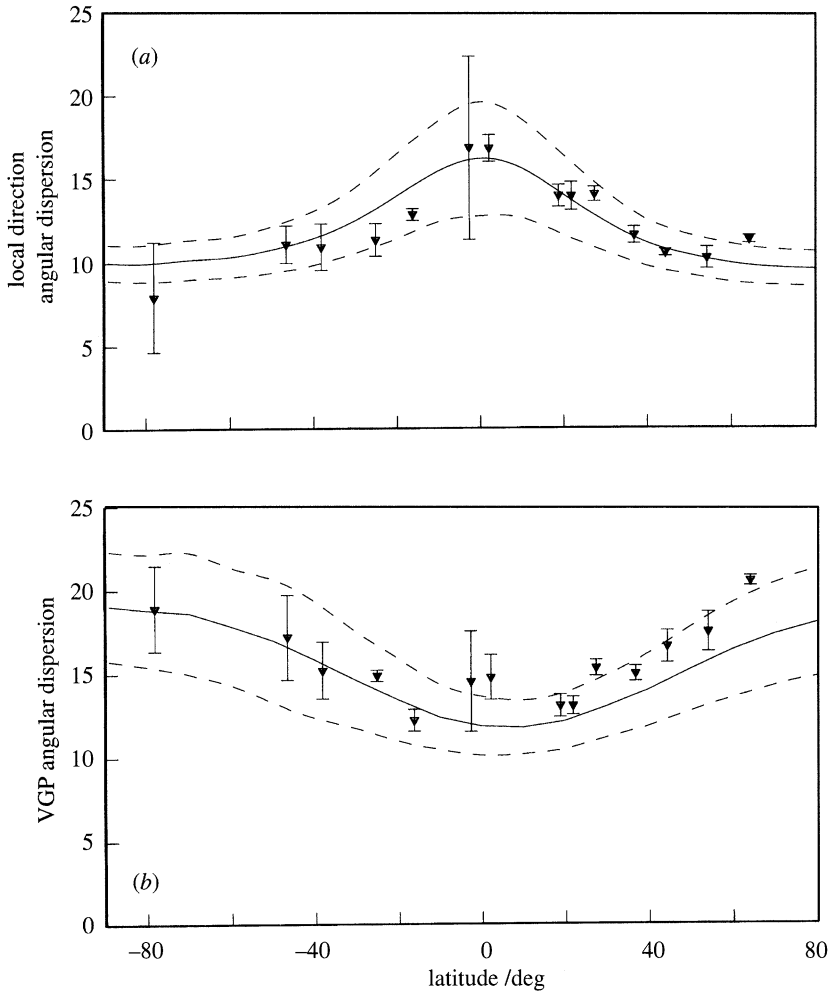

Figure 10. Latitudinally averaged VGP and direction dispersions for the data as in figures 8 and 9. Also shown is the corresponding variation predicted by a modified Constable & Parker (1988) model, in which the variance in the original model is reduced, but a component of local isotropic noise is added. The isotropic noise is represented by a Fisher distribution (see text) at each location superposed on the Constable & Parker (1988) model. Dispersions for the revised model are calculated every 10° of latitude with 1000 simulations per location. The solid line is the mean of the 1000 simulations, each with 15 points, and the dashed lines represent 95% confidence limits on the mean.

The problems inherent in figure 1 should now be apparent. First, the data distribution is constrained by the availability of suitable volcanics for palaeomagnetic work. Previous studies have assumed that PSV can be investigated by averaging scatter in the field directions and/or VGPs in latitude bands. This reduces the data coverage requirements but requires the time-averaged field to have certain geometric properties. Second, most previous PSV work has involved the use of VGP positions, which we have seen can incorporate several problems, not least of all the nonlinear mapping between field directions and VGPs. Third, the technique of combining Northern- and Southern-Hemisphere data may not be applicable for PSV studies where the time-averaged field requires a non-zero mean axial quadrupole term. Dispersion results for

the data presented in this paper are not symmetrical about the equator. The concerns discussed above indicate that, in many cases of PSV modelling, the apparent agreement between data and models can be misleading and is rather sensitive to the assumptions made during the data analysis.

4. Summary

We have presented a new database suitable for palaeosecular variation and time-averaged field studies. This database has been compiled using strict criteria regarding both the temporal extent of sampling and the data quality, and has superior spatial coverage to previous PSVL databases. Details of the contributing references are summarized on a regional basis in the appendix. Some properties of the database have been given, particularly those statistical parameters which are used in PSV work. Previous PSV models have been described, and we have compared the results from our new database with predictions of two of these models. Several problems with existing PSV models have been noted, mainly connected with the use of VGPs and assumptions concerning the time-averaged field. Earlier PSV models were based on databases quite different from that presented here, and our research indicates that many data included in these studies are unsuitable for PSV modelling. Existing PSV models cannot explain the statistical properties of the database presented here. Model G (figure 1, McFadden *et al.* 1988, 1991) does not accurately predict the dispersion and cannot account for Northern–Southern-Hemisphere asymmetry in the dispersion record. The Constable & Parker (1988) model does not predict the latitudinal dependence in the VGP dispersion and provides only poor agreement with the dispersion in the directions. Part of the poor agreement of this latter model with the data may be due to an inadequate average field model, this is supported by the VGP latitude and longitude distributions. The VGP longitude distribution obtained from this database has similar gross features to those observed in the distribution reported by Quidelleur *et al.* (1995), but it is much more homogeneous than the distribution reported by Constable (1992) using the Lee database alone. The main conclusion of Constable (1992) still holds – i.e. there is evidence for non-zonal structure in the time-averaged palaeofield (Gubbins & Kelly 1993; Johnson & Constable 1995). However, there is no longer an obvious link between PSVL VGP longitude distributions and the preferred VGP longitude bands observed in some field-reversal records (Clement *et al.* 1991; Tric *et al.* 1991; Laj *et al.* 1991). We have proposed that PSV studies should use the dispersion in the field directions rather than the dispersion in the VGP positions as a measure of temporal field variability. The main non-dipolar signal in the 0–5 Ma data recorded by lava flows is the far-sided effect; however, we have noted that the non-dipolar signal may be different for normal and reverse polarities. As a result, PSV studies need to investigate variations about the average field for the Northern and Southern Hemispheres, and possibly normal and reverse data, separately. This study emphasizes the need for an improved understanding of the time-averaged field, for both normal and reverse polarities, before we can understand the statistics of palaeosecular variation.

We thank Bob Parker and Guy Masters for helpful discussions and critical reviews of the manuscript. Two anonymous referees also provided useful suggestions which improved the paper. This work was supported under NSF grant EAR92-05653.

PHILOSOPHICAL TRANSACTIONS OF THE ROYAL SOCIETY A MATHEMATICAL, PHYSICAL & ENGINEERING SCIENCES

Appendix A. Contributing references

References contributing to the revised PSVL database are summarized and grouped by region. The database can be summarized on a regional basis in terms of the VGP positions. Figures 11–21 are stereo projections of VGP positions calculated for all the data in each geographical region. Previous studies have compared palaeomagnetic results from different continents and ocean basins, so we have tried to use similar regional divisions in analysing the data. As Iceland and Hawaii contribute 14.8% and 18.2% of the data, respectively, we have separated these data from the rest of the Pacific Ocean and Atlantic Ocean data. We also choose to display the data in terms of VGPs for comparison with previous studies. For each region, we show the individual flow VGPs (left-hand side of figures 11–21). For each PSV study, a mean VGP is calculated together with the corresponding α_{95} (α_{95} defines the 95% cone of confidence for the mean) and these mean VGPs are also shown for each region on the right-hand side of figures 11–21. In each of the figures 11–21 the left plot shows the individual VGP positions calculated for each group of data listed in table 2. The right plot shows the mean VGP position for each group together with the 95% cone of confidence for the mean (α_{95}). Filled circles represent normal polarity data, open circles represent reverse polarity data. Latitude grid lines are every 10°. Note that although VGP positions are given in many references, some were computed on hand calculators for the older studies and may be inaccurate by up to a few degrees. The VGP positions presented and discussed in this paper have been recalculated from the directional data; however, those in the on-line database are the VGPs quoted in the original references. Figure 22 summarizes the age distribution of the contributing data. A few poorly constrained age ranges have a maximum age slightly greater than 5 Ma, but we have retained these data on the basis that the most probable ages for these flows are less than 5 Ma. The majority of the data is of Brunhes age, as can be seen in figure 22. It should also be mentioned that in many cases where radiometric ages are available, the range of radiometric ages may not be entirely consistent with the polarity of the data; for example, a group of Brunhes age flows may have radiometric ages (including uncertainties) spanning 0.0–1.0 Ma, rather than the expected 0.0–0.78 Ma. We have retained the original radiometric ages in the database. A summary of each reference is given, where the code used in the first column of table 2 is provided together with the (sometimes abbreviated) title of the paper. The corresponding authors, journal, site location and age ranges are given in table 2. Pertinent field and experimental information from the original reference is reported. Reasons for excluding/including specific data are given and differences from the Lee database mentioned. If data from a particular reference were included in the original Lee database, an asterisk is placed before the reference code. For data referred to by both the Lee and McElhinny databases, the Lee code is given first in the description header, with the McElhinny code following in parentheses. References for which no summary is available are marked by a '$' sign in table 2. The descriptions below are in note form and are intended to serve solely as a guide to the database, not as a complete review of the contributing palaeomagnetic literature.

Africa

*** G14-52; (M35) Geophysical studies of North African Cenozoic volcanic areas. I: Libya**

Summary Paper part of a larger study to determine Neogene absolute motion of the North African plate. Sampled 70 volcanic units for combined K-Ar, palaeomagnetic study. Obtained a mean pole position significantly different (at 95% level) from

geographic pole, which may indicate insufficient temporal sampling. Four cores per unit, AF demagnetization performed. Radiometric ages, 0.4–2.2 Ma.

Database Ten normal polarity records (Site 22 removed from Lee database – only two samples). Three (10, 14, 20) reverse polarity sites removed from Lee database (only two samples per site), leaves 54 reverse records.

* G13-09; (M672) Palaeomagnetism and K-Ar ages of Ngorongoro caldera, Tanzania

Summary Sampled Gauss–Matuyama boundary and Matuyama epoch. 23 flows and one tuff sampled, five cores per unit. AF demagnetisation up to about 200 Oe generally sufficient to remove secondary magnetizations. Thermomagnetic properties investigated. K-Ar dating on one flow and tuff. Mean pole is displaced 10.5° from geographic pole but the 95% confidence cone in the mean is 11°. VGP dispersion is large and apparently non-Fisherian.

Database 12 Matuyama age records.

* G14-21,22,46; (M15) Palaeomagnetism of the Gulf of Guinea Province, West Africa

Summary Palaeomagnetic sampling carried out in three main areas: Cameroun, Fernando Poo and Sao Tome; all suggest no detectable movement of the plate relative to the geographic pole for the past 25 Ma. Sao Tome mostly basaltic lavas, but largely inaccessible. Fernando Poo young volcanic island with alkali olivine basalts. Cameroun has three main stages of volcanism exposed. Up to five cores per site collected, AF demagnetization up to 400 Oe. Palaeopole for Fernando Poo significantly different from geographic pole, even though all the flows sampled (and the whole island) are less then 700 000 years old.

Database *(a)* Cameroun: 15 Brunhes age records (sites 4, 13, 15, 29 removed from Lee database (low k). Site 29 added); (*b*) Fernando Poo: 38 Brunhes age sites (Sites 9, 30 removed due to two samples per site; sites 25, 36, 41 omitted due low k; site 36 added); (*c*) Sao Tome: 14 Brunhes age (sites 1, 45 removed, two samples per site). 9 sites with age range 2.5–4.0 Ma. 14 reverse polarity sites (site 20 removed, two samples per site; site 51 removed – intrusive).

Antarctica

M1319 Paleomagnetic investigation of some volcanics from McMurdo province, Antarctica

Summary Volcanism covers Gauss–Brunhes epochs. Total of 303 cores from 39 localities obtained. No evidence for tectonic disruption. Very few samples showed any change on AF demagnetizing, probably the result of little alteration in the extremely arid environment. Detailed results for each location given in paper. Mean VGP position is 86.6 °N, 334.8 °E with $\alpha_{95} = 6.6°$. Total dispersion of the VGPs is 23.7°, and the dispersion corrected for within-site scatter is 23.5°, with 95% confidence limits of 20.5° and 27.4°.

Database 18 records grouped in two locations (5, 13) of Brunhes/Jaramillo age.

Asia

* G9-06, G9-07, G9-08; (M409) Paleomagnetic investigation of Taiwan igneous rocks

Summary Paper deals with palaeomagnetic investigations in eight geologically different areas in Taiwan: data from only three areas could be used in the database. Laboratory methods included a.c. demagnetization up to 800 Oe of all the specimens, thermal magnetic treatment of selected samples and petrographic analyses.

Database (*a*) Tatun volcanic group: 27 N polarity mid Plio-Pleistocene andesite flows. Nine records removed from Lee database (only two specimens per flow). (*b*) Shiukuran River: 12 N polarity andesites of Plio-Pleistocene age. In the Lee database these were combined with Penghu Islands data although these two locations are more than 100 km apart. The 6 R polarity records in the *Lee* database were removed as they are Miocene age. (*c*) Penghu Islands: 7 R polarity Plio-Pleistocene basalts. N polarity Penghu Islands records removed from Lee database after separating from Shiukuran river data since there are only four suitable flows. (*d*) We also removed all data from Keelung area (6 N, 19 R polarity records) originally in Lee database since intrusives and extrusives were not distinguished.

Concern Lack of good age constraints.

C0001 Paleomagnetism of Pleistocence Usami volcano, Izu peninsula, Japan

Summary Palaeomagnetic study of a section of andesite flows and pyroclastic deposits at Usami volcano. Flow thicknesses generally 3–5 m. Probable that tilting of the strata occurred after emplacement and this is corrected for (based on field observations) in the final palaeomagnetic analysis. Two specimens from each site were stepwise a.c. demagnetized up to 480 Oe. Field intensity measured, standard thermomagnetic analyses performed and X-ray diffraction experiments carried out.

Database Five normal polarity, probably Brunhes but possibly Matuyama age, andesite flows included in database. Note that the data from this paper (Kono 1968) were combined with data from the following reference, C0002 (Kono 1971), and given an age range of 0–1.6 Ma.

C0002 Intensity of the Earth's magnetic field in geological time

Summary Palaeointensity study of flows from three locations: Hakone volcano (Izu peninsula), Mt Fuji volcano (Izu peninsula) and Kita-Matsuura basalts (north-west Kyushu). Experimental procedures applied as in previous reference, C0001. No record of post deposition tilting of strata.

Database One record from Mt Fuji, seven from Hakone. All Brunhes age normal polarity basalts, but combined with data from Kono (1968), so given collective age range of 0–1.6 Ma.

M1588 Palaeomagnetic study of the Ashitaka dike swarm in central Japan

Summary Hand samples collected from 35 narrow (0.2–4 m) dykes which form a radial swarm from Ashitaka volcano, Izu peninsula. Stepwise AF demagnetization up to 100mT. Mean direction determined using minimum dispersion criterion (i.e. mean direction given by the remanence at the demagnetization level which has the lowest dispersion, or equivalently the greatest precision parameter). All dykes inferred to be Brunhes age.

Database Include all data.

M1301 Palaeomagnetic results from Luzon and central Philippines

Summary Detailed study involving collection of 550 samples from 86 sites from the Philippine Arc. Ages span Jurassic to present and study aimed at investigating tectonic rotations of the islands in the Philippine Arc. Main conclusion of study applicable to this database is that there has been no rotation of the arc during the Plio-Pleistocene. Bedding corrections applied to older sites, but not required for late Miocene and younger samples. Many different lithologies sampled. Lab work involved AF demagnetization, Curie temperature analysis, thin sections, hysteresis measurements.

Database Only five of Plio-Pleistocene records suitable for inclusion in the database after discounting tuffs and sediments, and applying the criteria given in the main text to the tabulated results. All five are normal polarity basalt flows from the island of Mindanao. No detailed age information is available, so limits of 0.0 and 5.0 Ma had to be used.

Concern Lack of age constraints, small number of data.

Atlantic Ocean

* G14-17; (M13) Brunhes geomagnetic secular variation on Terceira Island, central North Atlantic

Summary At least six cores per igneous body taken from 33 bodies (flows and ignimbrites) yielding a mean VGP dispersion for the Brunhes of 13.9° with 95% confidence limits of 16.3° and 12.2°. Investigated effect of reducing number of specimens per flow on the estimate of within-site dispersion and concluded that for this particular study could have reduced sampling by about half without significantly affecting the results. Four stratovolcanoes (Pico Alto (PA), Cinquo Picos (PC), Guilherme Moniz (GM) and Santa Barbara (SB)) comprise most of the island, and are cut by morthwest–southeast trending fissures associated with the Terceira rift. Volcanics associated with PA mostly pumice, with few basaltic flows. More basalts associated with CP and GM, pyroclastics also associated with GM. SB intially developed as lavas and ash with some late stage pumice. 236 cores from 33 separate bodies oriented to $\pm 2.5°$ and with lateral separation typically > 10 m. Details of sampling sites given in their appendix. We assume tectonic corrections made to the slopes mentioned in their appendix. AF demagnetization up to 200 Oe and minimum dispersion criterion used.

Database Nine records (flows $1, 3, 6, 11, 16, 20, 22, 27, 32, 33$) removed from Lee database due to low precision parameter. Flow 4 removed since welded ignimbrite. Leaves 20 Brunhes age flows.

* G14-31; (M19) Brunhes epoch geomagnetic secular variation on Marion Island

Summary Palaeomagnetic survey of 30 Marion Islands' flows gives broad 95% confidence interval for Brunhes VGP dispersion. Marion and Prince Edward islands part of single volcanic platform. Marion island exposures alternate between effusive and explosive; the lavas are alkali basalts or trachybasalts. Older volcanic series has K-Ar dates of 100–300 ka and the younger series is < 23 ka. The two series are separated by a glacial period. 220 cores from 30 flows oriented to $\pm 2.5°$. AF demagnetization up to 200 Oe and minimum dispersion criterion used.

Database 15 contributing flows.

*** G14-39,64 (M25) Palaeomagnetism of the Canary Islands and Madeira**

Summary Palaeomagnetic results from 1144 specimens from 359 igneous bodies for the Pliocene, Pleistocene and Miocene give mean VGP positions not significantly different from axial dipole. K-Ar dates on 90 of the bodies. Geology in earlier references. The Pliocene data in this paper includes the Brunhes age data presented in Watkins *et al.* 1972. Samples collected during 1965, 1966, 1968. Cores oriented to ±3° and 2–8 collected per igneous body. AF demagnetization up to 300 Oe and minimum dispersion criterion used. K-Ar dating details in earlier references.

Database Data subdivided according to individual contributing islands: (*a*) all 14 N polarity Pleistocene Lanzarote records removed from Lee database (two samples per site); (*b*) 5 N Pleistocene Tenerife data removed (two samples per site), leaves 18 Brunhes records; (*c*) 18 N Pleistocene Hierro records removed (two samples per site), flow 28 (low k), leaves 10 Brunhes; (*d*) 2 N Pleistocene La Palma sites removed (flow 9, intrusive, flow 14, low k), leaves 14 Brunhes; (*e*) all N Pliocene data removed (mostly two samples per site); (*f*) 14 R Pleistocene Tenerife flows removed (two intrusive, others two samples per flow), six Matuyama left; (*h*) all remaining reverse data removed, mostly because only two samples per site.

M1404 Palaeomagnetism and rock magnetism of Fernando de Noronha, Brazil

Summary Pole positions obtained from seven basaltic sites from Quixaba Formation (3.4 ± 1.7 Ma, K-Ar) on Fernando de Noronha and from seven sites from Remedios formation (9.5 ± 1.1 Ma, K-Ar). Also sampled seven Cretaceous (28.7 ± 2.5 Ma, K-Ar) basaltic sites from mainland province of Fortaleza. 5–13 samples from each site. Pilot samples AF demagnetized up to 1000 Oe, other samples cleaned accordingly. Some Quixaba sites (55, 61 and 69, 70) gave directions not significantly different (F-test) and so were combined to give seven independent measurements in total. For the Remedios, two sites were rejected due to VGP latitudes $< 50°$, and an additional one site rejected due to contamination by VRM, leaving seven useful sites. Forteleza sites poor quality – large within site scatter and low remanence stability.

Database All seven Quixaba sites OK (N, basalts). Remedios mostly pyroclastics and intrusives, so unsuitable.

M799 Paleomagnetism and K-Ar ages of some igneous rocks from Trindade Island, Brazil

Summary Palaeomagnetic and K-Ar study of seven thin intrusive igneous units on Trindade Island support Gauss–Matuyama transition age of 2.41 ± 0.05 Ma. Island 1150 km off Brazil and 1800 km west of the mid-Atlantic Ridge. Pyroclastics, intrusives and extrusives. Oriented hand samples collected. AF demagnetizations, K-Ar determinations.

Database Five suitable normal polarity sites. Age range 2.3–3.3 Ma.

M1654 K-Ar chronology and palaeomagnetism of volcanic rocks in the Lesser Antilles Arc

Summary Detailed study of 16 islands in the arc. K-Ar dates for the outer arc are in range 38–10 Ma, for the inner arc they are less than 7.7 Ma. Only data useful here are from St. Vincent Islands. Flows sampled mainly associated with Richmond and Soufriere volcanic centres. Ages in range 0.29–2.85 Ma for dated samples. Both normal and reverse polarities sampled. AF demagnetization and optimum fields selected using criterion of minimum proportional change in magnetization vector between successive demagnetization steps. Rock magnetic studies done.

Database 9 N polarity records from St. Vincent. Age range 0.29–1.28 Ma but probably Brunhes.

M442 Palaeomagnetism of Atlantic Islands: Fernando Noronha

Summary VGP poles for nine sites from Quixaba formation (4 N, 5 R) and 15 from Remedios formation (11 N, 4 R). Some sites overlap with later study of Schultz *et al.* (1986). At least four cores drilled from each of 28 sites. NRMs measured. Paper states that there is no overprinting, so OK to use NRM. Four sites rejected due to poor quality data.

Database Quixaba sites 1–5 (R) and 7 (N) distinct from Schultz *et al.* (1986) sites. Although NRM, Schultz *et al.* (1986) added these results to their own so presume NRMs OK.

Australia

* G11-09 A paleomagnetic study of secular variation in New Zealand

Summary 22 Brunhes formations gave VGP scatter of 19.6° with 95% confidence limits of 16.2° and 24.7°, larger than model predictions at time of paper (1969) but comparable with studies at similar latitude in North America. Corresponding scatter in directions was 13.2° with 95% limits of 10.9° and 16.7°. Eight cores per flow. AF demagnetization.

Database 19 Brunhes records. Originally 21 in Lee database, but one record (NZ4) removed due to low VGP and another removed (NZ2) since > 300 km away from remaining sites.

* G13-11 Paleomagnetic secular variation from the newer volcanics of Victoria, Australia

Summary Study of 46 alkali olivine basalts from the newer volcanics, which are Pliocene to Holocene in age and outcrop over area of 25 000 km^2. The 25 N and 21 R sites showed no significant difference in VGP scatter (11.4°). Oriented hand samples with average of three samples per site. AF demagnetization.

Database All 46 sites originally in Lee database. Removed 3 N, 2 R records with only two samples per site. Remaining data subdivided into two locations: sites 27–36, 38 at 142.8 °E, 38.0 °S (5 N, 5 R); the rest at 144.5 °E, 38.0 °S (17 N, 14 R).

Europe

* G11-12; (M554) Etude paleomagnetique des basaltes du Plateau du Velay

Summary Both N and R polarities found in flows (basalts apart from one andesite). Stratigraphic dating indicates substantial volcanism during the Matuyama. Inferred that the N polarity rocks observed here are from either the Jaramillo event or the beginning of the Brunhes. Stepwise AF demagnetization to 400–600 Oe.

Database Seven normal polarity records (Brunhes/Jaramillo) – A2, B4, D1, D3, D5, D6, E3. 13 Matuyama R records

*** G12-09; Paleomagnetic secular variation study, the Massif Central, France**

Summary VGP scatter from 31 Brunhes-age lava flows is 15.2° referenced to an axial dipole mean. Confidence limits are 18.4° and 12.9°. Most Brunhes samples from Chain des Puys (near Clermont-Ferrand), some from the valleys and tributaries of the Ardeche. Some pre-Brunhes samples from Chain des Puys and southwest of Montpellier. Eight cores per flow, with maximum lateral separation of a few hundred m. Progressive AF demagnetization on one specimen per core 25–800 Oe. Compare sequential directions during demagnetization for each core from single flow and omit specimens which do not appear to reach a stable remenanence. Of 33 original flows 31 retained.

Database All 31 flows OK. 26 grouped as one location, five as another, as flows separated by more than 100 km.

*** G10-09; (M517) A palaeomagnetic study of Quaternary volcanic rocks from Turkey**

Summary Brunhes and Matuyama epoch volcanics give mean VGP consistent with a GAD at the 95% confidence level. Estimated standard deviation in directions is 10.0–11.5° for Brunhes (depending on whether used simultaneous or successive two-tier analysis) and 16.2° for Matuyama. At least four oriented hand samples per flow. Thermomagnetic and ore microscopy studies. AF demagnetization.

Database 16 suitable Brunhes flows but separated by several hundred kilometres. Use ten records which can be grouped into two locations with five records per location

M1072 PSV studies of the Brunhes in the volcanic province of the East-Eifel, Germany

Summary Mean pole derived for Brunhes from 31 independent events consistent with the GAD hypothesis. VGP dispersion is 15.1°. Palaeomagnetic samples from 46 sites, 6–17 cores per site each giving 2–3 specimens. Several sites dated radiometrically as well as stratigraphically. 2–3 samples per site AF demagnetized up to 700 Oe. NRM stability varied; classified four types, relate to grainsize. Most VRM removed by 100–200 Oe fields. Used a stability index (Symons & Stupavsky 1974) to investigate best demagnetization level – all other samples for given site demagnetized in this range. Take site mean direction from the stable region at alternating fields yielding minimum α_{95}. Several sites give directions not significantly different (F-test), combining these yielded 31 independent sites.

Database Site EEL5 omitted due to low VGP latitude (52.6°), leaving 30 Brunhes age sites.

M1513 Palaeomagmagnetic investigation of Quaternary West Eifel volcanics (Germany)

Summary 64 VGPs gave asymmetric longitude distribution with low-latitude VGPs ($< 60°$) concentrated in the longitude band 30–120° E. Mean VGP significantly different from GAD. Anomalous VGPs possibly represent an event/excursion within the Brunhes epoch. Volcanism began during the Pleistocene with the main activity at 0.7 Ma. 85 sites sampled representing 73 of the West Eifel eruption centres. Sites

PHILOSOPHICAL TRANSACTIONS OF THE ROYAL SOCIETY A MATHEMATICAL, PHYSICAL & ENGINEERING SCIENCES

in lava flows, dykes, scoria cones, sill-like flows, plugs and two tuffs. A few samples thermally demagnetized. AF demagnetization of three or more specimens per site up to 1200 Oe. Remaining specimens demagnetized in 3–5 steps after a stable direction reached in pilot samples. Sites suspected from being from same eruption centre subjected to F-test and directions combined if necessary.

Database Sills excluded leaving a total of 37 Brunhes sites, five are combinations of more than one original site.

* G12-22; (M638) Secular changes, polarity epochs & tectonic movements, Hungary

Summary Palaeomagnetic investigations of Plio-Pleistocene basalts, Miocene andesites, Lower Cretaceous volcanics. Results described separately for each age group with emphasis on the correlation of magnetic polarity with the geology. Six cores per outcrop taken. Stepwise AF demagnetization in fields increasing by 100 Oe. Site mean direction computed for the demagnetization stage for which the dispersion on a stereo plot was estimated visually to be a minimum. Thin sections and thermal demagnetization also. No significant post deposition tectonics.

Database Six R records from Transdanubia included (N polarity data OK but only four records).

M34 Evolution of a section of the Africa-Europe plate boundary: evidence from Sicily

Summary Palaeomagnetic data from Upper Cretaceous, Neogene and Quaternary volcanics indicates that Sicily is part of the African plate which collided with the European plate in Middle Miocene times. The geochemistry suggests different episodes of volcanism since the late Tertiary. Eight Upper Cretaceous dykes (Capo Passero) and ten Plio-Pleistocene lavas from Mt Ilbei. The Mt Ilbei lavas vary from allkali basalts to tholeites – uncertain whether this is due to different degrees of partial melting at the same depth or partial melting at different mantle depths. Field and lab details omitted here except that overprints generally removed by a 150–200 Oe field. AF demagnetization resulted in lower scatter without significantly changing the mean directions.

Database D, I only given to nearest degree but data retained as overall analysis seems OK. Six suitable R Plio-Pleistocene Mt Ilbei sites, only 4 N so N data omitted. Four of the R sites are dated: three are Matuyama, the fourth is Gauss, implying an incorrect age or flow from a R polarity event during the Gauss.

Hawaii

M285 Paleomagnetism of Hawaiian lava flows

Summary 148 flows from the Island of Hawaii, with ages from around 300 BP to 350 ka. 112 flows have multiple samples. Data are from five different volcanic series on the island, some of whch erupted repeatedly over very short time intervals and thus provide poor samples of the range of directions expected for PSV. Original age estimates provided in this paper are largely based on plausibility arguments, and the data presented in McWilliams *et al.* (1982) supercedes these. No evidence for

PHILOSOPHICAL TRANSACTIONS OF THE ROYAL SOCIETY A MATHEMATICAL, PHYSICAL & ENGINEERING SCIENCES

tectonic tilt; rock magnetic studies used to infer that the NRM represents the field at the time of cooling of the lava flows; AF demagnetization did not reduce scatter. The volcanic series are: (1) Puna, 18 flows, age range 300–500 BP, based on C14; (2) Kahuka, 28 flows older than 10 ka (based on stratigraphy to an ash flow) believed to represent a time interval of 5000–75 000 years (based on amount of dispersion in data); (3) Hamakua, 11 flows older than 10 ka, believed to sample only 100–200 years because of the low dispersion, but no data is available for direct comparison; (4) Ninole, 25 flows older than 10 ka; (5) Pololu, 29 flows with K-Ar ages in the 200–300 ka age range.

Database Puna and Hamakua series omitted (insufficient temporal sampling). Others included.

M667 Paleomagnetism of lava flows from Kauai, Hawaii

Summary Study of 571 cores from 120 flows indicated: (i) far-sided mean palaeopole; and (ii) low secular variation. Ages range 3.5–5.6 Ma. Eight samples per flow in the Makaweli formation and five per flow in the Napali formation and Koloa volcanic series. AF demagnetization up to 400 Oe.

Database 46 normal and 42 reverse flows. Single samples and asterisked data in paper omitted. Latitude in Lee database corrected to 22.0 (from 20.0).

M31 Paleomagnetism of volcanic rocks from Niihau, Nihoa and Necker Islands, Hawaii

Summary Sampling of 39 flows gave far-sided palaeopole for Niihau, although that for Nihoa was very close to geographic axis. Necker island gave low-latitude VGPs. The VGP dispersion is low, consistent with low dispersion observed at other Hawaiian islands (see, for example, the above reference). Eight cores per flow on all three islands. AF demagnetization.

Database Seven flows from Necker excluded since 10 Ma. Nihoa: 14 flows, all about 3 Ma, all normal. Niihau: 16 flows – Kieke series 0.3–0.7 Ma (11 normal flows); Paniau series 3 Ma (five reverse flows).

M42 K-Ar ages and paleomagnetism of the Waianae and Koolau volcanic series, Oahu

Summary Waianae active from 3.6–24.0 Ma. 99 flows sampled from the Waianae and Koolau series. Stepwise AF cleaning. Five low-latitude VGPs possibly indicate an excursion.

Database 31 N, 27 R from Koolau series (2.6–1.8 Ma). Also 33 R, early Matuyama age.

C0003 Paleointensities from C14 dated flows on Hawaii and the Pacific non-dipole low

Summary Palaeointensity and directional data from nine radiocarbon-dated lava flows on Hawaii; age range 2600 BP to at least 17 900 BP. 2600–4000 BP flows yield high VDMs relative to global average. Angular dispersion for this subset is 15.5° (high compared with whole data set). At 18 ka there is a low measured VDM with unusually shallow inclinations, while around 10 ka, the VDMs are close to the global average values. Comparison made with other Holocene volcanic series and historic flows.

Database Results from seven reliable flows included

PHILOSOPHICAL TRANSACTIONS OF THE ROYAL SOCIETY A MATHEMATICAL, PHYSICAL & ENGINEERING SCIENCES

M668 Paleosecular variation of the Honolulu volcanic series, Oahu, Hawaii

Summary 25 flows from the Honolulu series on Hawaii sampled. AF demagnetization. K-AR ages from 30–850 ka, with some evidence that the upper part of the series is < 70 ka and the older is 350 ka.

Database 25 N flows.

Iceland

*** G16-19,20,29,30; (M1139) Upper Miocene and Pliocene geomagnetic SV, West Iceland**

Summary Study of VGP dispersion from 362 flows extruded at approximately regular rate. Used to extend geomagnetic polarity scale back to 6.5 Ma. Geological, stratigraphic details in McDougall *et al.* (1977). Stratigraphic column sampled about 3.5 km and covers period 1.6–6.7 Ma. Flow thicknesses vary considerably and some have been affected by recent hydrothermal alteration. Intrusives occupy only a small percentage of exposed volcanic pile. Lavas dip between 2–8° to the southeast except in one area where they dip eastward. Extensive normal faulting parallel to strike of flows and some faulting perpendicular to strike. AF demagnetization up to 200 Oe. K-Ar dates. Paper concludes that there has been no long-term changes in inclination over the 6.7–1.6 Ma period in contrast to a previous study by Wilson & McElhinny in east Iceland (1974) which suggested an increase in inclination over the same period. Also conclude the mean VGP positions for four polarity epochs are almost identical, suggesting similar average field structure for both polarities.

Database Original data from this paper was reanalysed by Kristjansson, who made tectonic corrections and excluded certain data based on high values of within-site dispersion. We updated the Watkins *et al.* (1977) data in the Lee database with this revised Kristjansson data (Kristjansson 1987; personal communication with C. Constable): (*a*) Normal polarity, 52 Gauss flows (2.4–3.4 Ma), 29 Gilbert (1.8–2.4 Ma) flows; (*b*) Reverse polarity, 68 Gilbert (3.4–5.0 Ma), 12 Gauss (2.4-3.4 Ma) flows, 8 Matuyama (1.57–2.4 Ma) flows.

M1496 Stratigraphy and paleomagnetism of the Esja, Eyrarfjall and Akrafjall mountains, southwest Iceland

Summary Mapping and sampling of a 2.1 km section (353 igneous units) in southwest Iceland spanning 4.2–1.8 Ma and incorporating more than ten glaciations. Mean field consistent with a geocentric axial dipole. Regional dip is 5–8° southeastwards, volcanic activity suggested to be fairly constant over the past 7 Ma. Area mapped is bisected by a major fjord, and some difficulties in correlation of strata across it. Most igneous units are basaltic, several glacial horizons. Stratigraphy confirmed by K-Ar dating. At least three cores per site drilled, AF demagnetization up to 200 Oe, minimum dispersion criterion used. 77 flows considered to overlap in time from geological correlations, details of overlaps given in reference.

Database Only one flow used where possible temporal overlap occurs, as defined in paper: (*a*) Normal polarity, 65 Gauss flows (2.4–3.4 Ma), 10 Matuyama age flows (1.8–2.4 Ma); (*b*) Reverse polarity, 16 Gilbert (3.4–4.0 Ma), 15 Gauss age (2.4–3.4 Ma) flows, 103 Matuyama (1.8–2.4) Ma flows.

*** G14-40 A detailed survey of the type location for the Gilsa geomagnetic polarity event**

Summary 163 cores from 40 flows in three distinct sections of Jokuldalur, Iceland. No mention of tectonic corrections. Conclude that Gilsa and Olduvai cannot be distinguished as distinct normal events within the Matuyama reverse epoch.

Database 19 reverse polarity Matuyama age flows.

Indian Ocean

*** G14-24; (M16) Paleomagnetism and K-Ar Age of St. Paul Island, southeast Indian Ocean**

Summary 135 cores from 18 separate bodies give an estimate for VGP dispersion for St. Paul Island greater than that for Amsterdam Island. St. Paul Island is a volcanic cone with circular central caldera breached to the sea by a large normal fault. It lies 3 km southeast of the mid-ocean ridge axis. Core complex is composed of pyroclastics and is overlain by tholeiitic flows. Up to eight cores drilled from each of 15 flows and three intrusives. Samples oriented to ±2.5°. AF demagnetization up to 200 Oe. Fresh unaltered samples from three flows in known stratigraphic sequence selected for K-Ar dating. Age estimates range from 0.01–0.64 Ma.

Database 14 suitable Brunhes age records. Three intrusives are not distinguished from the flows, but included as only three of them.

*** G14-27; (M18) Brunhes epoch geomagnetic secular variation on Reunion Island**

Summary VGP dispersion estimated as 17.7° with 95% confidence interval of 14.4–22.8°, based on at least seven samples per flow from 21 flows. Within each flow lateral separation of cores 5 m. Suggest that Brunhes SV higher than present which could be due to inadequate temporal distribution of data or to real SV changes. Also detect a large excursion at 0.51–0.61 Ma. AF demagnetization at 100 and 200 Oe, and minimum dispersion criterion used.

Database 17 flows with VGP latitude $> 55°$.

*** G14-05/23; (M4) Age of the Comore Islands, west central Indian Ocean**

Summary Data from Grande Comore, Anjouan, Mayotte give K-Ar ages in range 0.01–3.65 Ma, with age increasing southeastwards along the chain. Mean VGP for each island not significantly different from axial dipole at 95% level. No raw data published in this paper. Data from Grande Comore, Anjouan published in Watkins *et al.* (1972).

Database 23 Brunhes age flows from Anjouan, 12 Brunhes age flows from Grande Comore.

*** G14-28/29; (M11) Brunhes geomagnetic secular variation – Indian and Atlantic Oceans**

Summary Data from 401 igneous units (more than half previously unpublished) divided into first- (more than four samples per flow) and second-order data (no requirement on the number of samples). Both data sets indicate that VGP dispersion increases with latitude. Could not reject Pacific non-dipole low hypothesis. Consider

PHILOSOPHICAL TRANSACTIONS OF THE ROYAL SOCIETY A MATHEMATICAL, PHYSICAL & ENGINEERING SCIENCES

Indian Ocean data here – see Atlantic section notes for the Atlantic data from this paper. (1) Comore Islands – Anjouan, Grande Comore. Samples from these two of the four Comore Islands; 23 samples from Anjouan from the younger flows – 6 are melanocratic-ankaramitic, the remainder are basaltic; 14 samples are from Grande Comore – five from fissures in the northern volcanic centre and nine from the west and central coasts which are ankaramites or feldsparphyric flows from fissure eruptions. Inferred that this data is also that used by Hajash & Armstrong (1972), but the raw data is not published in Hajash & Armstrong (1972). This paper infers Brunhes age based on stratigraphy and polarity, which is consistent with the one radiometric age reported in Hajash & Armstrong (1972) for Grande Comore (0.01 ± 0.01 Ma) and the one normal polarity age reported for Anjouan (0.39 ± 0.2 Ma). (2) Amsterdam Island: Lies on transform fault, young-looking volcanic cone. 12 flows sampled. (3) Crozet Islands – Possession and East Island: Possession Island is the largest of the Crozet group. Series of horizontal to sub-horizontal basaltic flows at surface; similar geochemically and geomorphologically to East Island. K-Ar dating places Brunhes–Matuyama boundary in the lower part of three of the sequences sampled on Possession. All flows from East Island from Brunhes. 43 flows sampled on East Island (mostly one sequence) and 38 on Possession. Data presented in this paper collected over five years. Number of specimens per body varies. Orientation accuracy 2.5°. One specimen per core AF demagnetized at 100, 200, 300 Oe and mean direction computed using minimum-scatter criterion.

Database (a) Crozets (Possession) – 32 Brunhes (assume no overlap of different sequences); two low-VGP latitude sites removed and another with only two samples removed; (b) Crozets (East) – 37 Brunhes flows, three low-VGP latitude sites removed.

Concern Amsterdam Islamd data was removed (11 records) from Lee database because of possible overlap with that in Watkins & Nougier (1973). Lower precision parameter associated with some records, but these records retained due to extensive study in this area.

M17 Excursions and secular variation during the Brunhes in the Indian Ocean

Summary 33 flows on Amsterdam Island sampled, all Brunhes age. Six flows record 50–80° latitudinal departure of the VGP from the present geographical pole – probably recording one or two excursions. Remaining 27 lavas give a VGP angular standard deviation of 14.6° with 95% confidence interval of 12.5–17.7°. Amsterdam Island comprises an older volcanic episode in the southwest of the island and younger extrusives elsewhere. Lavas range in composition from olivine tholeites to high alumina basalts. No radiogenic ages, but geology consistent with Brunhes age. 237 cores, 2.5 cm diameter from 33 lava flows. Cores oriented to ±3° *in situ*. Sites 11, 20–29 from the geomorphologically older parts of the sland. Sites 30–33 from recent summit crater and remaining sites from the younger flows draping the old volcanic center. AF demagnetization at 100 and 200 Oe. Flows 2, 13, 17, 18, 19, 24 have VGP latitudes in the range 24.5–32.2°, possible evidence for excursion(s).

Database Flows 1, 3-10, 12, 14-16, 20,21,23, 25, 27-33 OK. All Brunhes.

C0004 Paleointensity recorded by two late Quaternary volcanic sequences, La Reunion

Summary Investigation of two sequences associated with the volcano Piton de la Fournaise. One sequence gave radiometric dates of 5–12 ka, the other 82–98 ka. Detailed rock magnetic studies and Thellier palaeointensity experiments performed. VDMs show very little variation for youngest sequence and are comparable with worldwide VDM fluctuations for this period. Data from older sequence are the only data for this time interval and gave VDMs comparable with younger sequence. Results indicate intermittent emplacement of flows.

Database 27 Brunhes age flows.

*** G14-48; (M32) Age and duration of the Reunion geomagnetic polarity event**

Summary Reunion polarity event is dated at 2.02 ± 0.02 Ma with a duration of 10–50 ka. Omit event data in case of insufficient temporal distribution for estimation of secular variation. Two sequences sampled: Grande Chaloupe and Riviere St. Denis. Riviere St. Denis (RD) section stratigraphically lower than Grande Chaloupe (GC) section. GC – three oriented samples from each of seven flows. RD section – three cores per flow from 29 flows. Oriented to $\pm 3°$. AF demagnetization up to 300 Oe. K-Ar dates for eight of the flows. Lowest two samples in GC section normal polarity, next had random magnetization, upper four reverse polarity. 16 lower samples of RD section reverse polarity, next 11 normal, top transitional. Presumably seeing Matuyama to the end of Reunion in RD.

Database 13 R magnetized flows of RD section. Omit N data (Reunion) due to insufficient temporal sampling. Omit GC section since insufficient stable polarity data.

North America

*** G11-08 Paleomagnetism, K-Ar ages and geology of Valles Caldera rhyolites, New Mexico**

Summary Rhyolites and tuffs of Valles Caldera sampled to compare with previously established geomagnetic polarity timescale. Bandelier Tuff deposited about 1.4 Ma ago, rhyolites subsequent to this – both Matuyama and Brunhes epoch. AF demagnetization. K-Ar dates.

Database Six Brunhes-age normal-polarity rhyolites suitable.

*** G14-33; (M20) Paleomagnetic investigations of Tertiary and Quaternary igneous rocks**

Summary Investigated palaeomagnetism of volcanics from the Valley of Mexico, partly to study any possible relationship between oxidation state and magnetic polarity (did not find any). Use the frequency of polarity changes observed to establish the temporal distribution of their sampling. Plio-Pleistocene data is from the Chinchinautzin volcanic group. Valley of Mexico is a basin surrounded by volcanic rocks Upper Oligocene to Recent in age. Little published on the geology of the Valley. Relevant formation here is the Chinchinautzin group (Upper Pliocene – Pleistocene

to Recent). 5–10 cores per site. Two specimens per site AF demagnetized up to 1200 Oe. Remaining samples demagnetized at the level at which stable remanence reached in the pilot samples and at one level higher. Mean directions then taken from the demagnetization stage which gave the highest magetization value and the smallest cone of confidence.

Database Removed flows 11, 13, 22, 26, 27, 32 leaving 30 Brunhes records. Only a handful of these data are used in a later compilation by Herrero-Bervera *et al.* (1986) – not clear why.

M1429 Negative inclination anomalies from the Medicine Lake Highland Lavas, N. Ca

Summary Data from 21 Quaternary age flows from Medicine Lake Highlands give a mean VGP at 78.0 °N, 42.4 °E – far sided and right-handed. Mean inclination is 49.3°, 12° shallower than predicted by a GAD. Volcanic activity (recent) is dominantly andesitic with some high-alumina olivine tholeiites and some low-Si andesite. Most flows 1–5 ka old, all the volcanics probably less than 100 000 years old (K-Ar ages). No maghaemite observed in the 21 Brunhes age flows sampled, suggesting post-solidification oxidation not a significant factor. 6–8 cores per flow. Care taken to sample only sites which had not undergone post deposition rotation. Stepwise AF demagnetization (25–800 Oe) on several samples, NRM generally very stable. Remaining samples demagnetized at 200 Oe.

Database Remove 1, 4, 17, 20 due to low value of precision parameter. Remove flow 7 due to low VGP lat. Leaves 16 records.

M1749 Palaeomagnetic results from rocks from the East trans-Mexican volcanic belt

Summary East trans-Mexican volcanic belt classified into four geological units. 55 sites sampled, AF demagnetized. Used stability index (Symons & Stupavsky 1974) to establish optimum demagnetizing field. Rock magnetic studies done. Sites 1–33 of quaternary age and thus of interest here.

Database 20 Brunhes age records suitable.

C0005 Paleomagnetic directions from the Iztaccihuatl volcano, Mexico

Summary This 1985 paper refers to a 1971 paper by the same author for details of palaeomagnetic sampling and lab work. AF and thermal demagnetization. Magnetic carrier essentially pure magnetite, flows normally magnetized. 24 flows yield a value for VGP dispersion consistent with that expected for Brunhes epoch. Results consistent with K-Ar dates for volcano.

Database 21 of the 24 flows suitable.

C0006 Paleomagnetism and K-Ar ages of volcanic rocks from Long Valley Caldera, California

Summary K-Ar dates indicate post-caldera eruptions began about 0.73 Ma and continued intermittently until about 50 000 years ago. Mean pole position from 33 volcanic units is indistinguishable from the geographic pole. VGP scatter about this mean pole is 16.0° with 95% confidence limits of 13.6° and 19.3°. Rocks sampled mostly rhyolities or basalts with 3–8 cores per site. AF demagnetization performed with optimum field chosen on basis of behaviour during demagnetization.

PHILOSOPHICAL TRANSACTIONS OF THE ROYAL SOCIETY A MATHEMATICAL, PHYSICAL & ENGINEERING SCIENCES

Database 33 Brunhes age flows (two flows excluded on the basis of low k).

C0007 Magnetostratigraphy and secular variation at Level Mountain, North British Columbia

Summary Results from 50 flows indicate eruptive behaviour began about 6.5 Ma and continued intermittently until very recent times. Most flows from stable polarity periods, but two record Gauss/Matuyama transition (as confirmed by K-Ar dates) and four possibly represent an excursion during the early Gauss. Average VGP position not significantly different from geographic pole, but is near-sided rather than far-sided. VGP scatter (about the mean direction) is 21.9° with 95% confidence limits of 19.9° and 24.4°. Two distinct sections, separated by 10 km sampled. Field evidence suggests sections do not overlap and there is no significant hiatus between them. AF demagnetization and minimum dispersion citerion used.

Database Only 11 suitable flows as all of section A may be > 5 Ma.

Concern Flows span age range 0–5 Ma so may be insufficient temporal sampling of each epoch.

M713 Evidence for excursions and secular variation from the Wrangell Volcanics, Alaska

Summary Sampled 36 late Tertiary (3–4 Ma) flows from three sections of Wrangell volcanics. Data from one section purely from an excursion (11 flows); from another (16 flows) is partly excursion, partly stable polarity; from another all stable polarity (9 flows). All stable polarity data is normal – Gauss epoch. Exclusion of excursion data yields value for PSV consistent with model predictions (14.0° with respect to the geographic north pole). Age of all three sections 3.4 Ma. 3–7 cores per flow. Stepwise AF demagnetization. For section with some excursion data & some stable polarity data pilot AF demagnetization was performed on 24 samples from 13 of the 16 flows and a value of 380 Oe chosen for blanket demagnetization of remaining samples. Since fewer samples collected from other two sections, one specimen per sample demagnetized until an end-point reached (below 340 Oe). Mean direction calculated using minimum dispersion criterion.

Database All nine flows from Air II location OK.

Concern Secular variation estimate may be less reliable due to limited temporal data distribution.

*** G9-13 Paleomagnetism of Pliocene Basalts from the southwest USA**

Flows from Rio Grande Gorge near Taos, New Mexico and near Flagstaff, Arizona sampled. Taos plain covered by Tertiary-Quaternary olivine basalts – 14 flows and two baked sediments cored. Seven basalts and two baked sediments sampled near Flagstaff. Rock magnetic studies and AF demagnetization performed. Early study (1967), so just interested in detecting reversals and investigating general magnetic stratigraphy.

Database Data only given to nearest degree but otherwise OK. Arizona data removed since only four sites. Two sub-sequence flows (Rio Grande) removed since may overlap main sequence. Leaves nine records with K-Ar dates in range 3.62–4.38 Ma.

PHILOSOPHICAL TRANSACTIONS OF THE ROYAL SOCIETY A MATHEMATICAL, PHYSICAL & ENGINEERING SCIENCES

C0008 Revised paleomagnetic pole for the Sonoma volcanics, California

Summary Study is an update of a 1972 study in the same area by Mankinen. Data from 25 flows yields a mean VGP position significantly different from the present day geographic pole. It is speculated that this is due to insufficient sampling of PSV rather than a different average field direction. VGP scatter is 18.6° with 95% confidence limits of 15.4° and 23.1°. Results not significantly different from those from the earlier 1972 study. Data spans 8–3 Ma. AF demagnetization.

Database 13 andesite flows from Andesite Peak, spanning 4–5.5 Ma.

C0009 Paleomagnetism of Plio-Pleistocene Louisetown formation, Virginia City, Nevada

Summary 61 flows sampled and their remanence directions fall into two distinct groups, both different from those predicted by an axial dipole field. One set of flows probably represents a polarity transition, the remaining flows suggest the late Pliocene field was significantly different from an axial dipole field. Six cores per flow, AF demagnetization, rock magnetic studies.

Database 6 R polarity flows from Carson Range and Truckee Basin suitable.

Concern No detailed age information (0–5 Ma).

Pacific Ocean

* G14-35; (M22) Palaeosecular variation of the geomagnetic field in the Aleutian Islands, Alaska

Summary Palaeomagnetic samples taken from six Aleutian Island sites to investigate the geographical limits of the low SV observed in the Pacific in other studies. Angular standard deviation in field directions is 10.8°, compatible with other low values from the Pacific region. Data from all sites need to be combined to obtain reasonable SV estimate. Age range of flows is late Tertiary to Quaternary. At least five cores per flow. AF demagnetization. Individual site descriptions given.

Database 53 N polarity flows, 8 R polarity flows.

Concern Lack of age information.

* G14-09; (M8) Paleosecular variation of lavas from the Mariana in the Western Pacific

Summary Study of 24 flows from Pagan Island gave a mean VGP consistent with GAD. Estimate of VGP dispersion of 6.2° with 95% confidence limits of 5.2° and 7.8°. Conclude either insufficient temporal sampling, or there is a Pacific dipole low, or a belt of low latitude VGP dispersion. Note that the authors could not obtain radiometric dates or get a reliable palaeointensity estimate (Thellier method). Brunhes age is inferred based on geology and polarity. Seven cores per flow taken for 22 of the flows and six cores per flow for the remaining two flows. Time span = historical (1925) – mid/late Quaternary. AF demagnetization performed up to 200 Oe, minimum dispersion criterion used.

Database 23 flows of inferred Brunhes age.

PHILOSOPHICAL TRANSACTIONS OF THE ROYAL SOCIETY A MATHEMATICAL, PHYSICAL & ENGINEERING SCIENCES

*** G15-14; (M741) Paleomagnetism and secular variation of Easter Island basalts**

Summary Study of 65 Brunhes age flows. Mean VGP not significantly different from GAD at 95% confidence level. VGP dispersion estimated to be 12.8° with upper and lower limits of 14.8° and 11.3°; consistent with, but less pronounced than, the low SV observed at Hawaii. Lower latitude VGPs cluster in longitude range 90–150° – possible excursion? Lavas intermediate between island tholeiites and alkali basalts and difficult to correlate across the entire island due to volcanic vents and pyroclastic centres. Three major volcanic episodes (and volcanoes) recognized: the youngest (<= 0.24 Ma) is sampled here from outcrops along sea cliffs. Four samples per flow collected. AF demagnetization performed up to 800 Oe on at least two specimens per flow. Directions in about $\frac{2}{3}$ of 65 flows changed little on demagnetization.

Database 53 Brunhes age flows.

*** G14-75; (M45) PSV on lavas from Norfolk & Philip Islands, southwest Pacific**

Summary Samples from 87 sites on the two islands gave a mean VGP dispersion of 7.5° and a mean VGP 14° away from rotation axis. Volcanism concentrated in two episodes – one at 3.05 Ma and the other between 2.8 and 2.35 Ma. Low VGP dispersion could be due to insufficient temporal sampling rather than Pacific dipole low. Norfolk island comprises basalts and tuffs, generally flat-lying or with an original dip of a few degrees. Flow thicknesses are 1–30 m. K-Ar dates indicate volcanism over period 3.1–2.35 Ma. Earliest flows during Mammoth reverse event (3.05 Ma), remaining flows span late Gauss and early Matuyama (2.75–2.35 Ma). Philip Island about 6.5 km south of Norfolk Island. Mostly tuffs but some basalts. K-Ar dates indicate volcanism occurring in latter part of Gauss (2.8–2.6 Ma). Assume authors just collected from basalts. Mostly only two samples per site. AF demagnetization in fields 50–600 Oe.

Database No VGP latitudes given in paper. 25 N, 12 R polarity records suitable.

Concern Possibly insufficient temporal sampling of data.

M663 Paleomagnetism of San Cristobal Island, Galapogos

Summary Island is most easterly of Galapogos and comprises large volcano in the southwest and flows and small cones in the northeast. Surrounding seafloor estimated to be 9–10 Ma. Minimum age of island based on R magnetized samples from south part of island is 0.7 Ma. Samples from north coast give a VGP dispersion of 11.3°, consistent with SV models. Sampling confined to 27 sites on north coast (could not land on south coast); 24 are from Brunhes. In paper sites, assigned an 'age group' (0–4) based on relative degradation of flows from field observations and air photos. Eight samples per site. Most cores drilled in or near the intertidal zone; almost none of samples affected by rotation during cooling and/or lightning. Orientation accuracy 2°. Specimens from 12 sites AF demagnetized in fields 12.5–800 Oe. In general fields of 50–100 Oe raise precision parameter to at least 380. Doesn't say if/why didn't clean all samples. Some flows may be very closely spaced in time, so number of independent Brunhes sites reduced to 17, retaining the more accurate of overlapping flows. Dispersion = 11.3°.

Database Appear to be 18 records in table rather than the 17 mentioned in the text. Brunhes age. Minimum VGP latitude = 66.9°. Omit reverse data points since only two.

PHILOSOPHICAL TRANSACTIONS OF THE ROYAL SOCIETY A MATHEMATICAL, PHYSICAL & ENGINEERING SCIENCES

C0010 Geomagnetic reversals from volcanic islands of French Polynesia: (1) Huahine

Summary Aim of paper is to look at structure of the field during a reversal. Sampling done in two field seasons. First season involved a general survey around Huahine at same locations as those visited by Duncan (1975), so older data replaced from this reference. Second field season involved detailed study of Mahuti Bay on the southern part of Huahine Iti. No tectonic corrections necessary. Five new K-Ar ages in range 2.91–3.08 Ma. Most transitional flows observed in Mahuti area, but no reverse directions sampled indicating most of the volcanic activity on Huahine occurred during the Gauss normal polarity epoch. Some directions close to normal or reverse field directions had low palaeointensities – authors suggest these data actually indicate a transitional field. Flows that record the same average field direction grouped together.

Database Data for Huahine in Duncan (1975) and Lee database replaced with data from this paper. 32 normal polarity flows suitable: Gauss age.

C0011 Geomagnetic reversals from volcanic islands of French Polynesia: (2) Tahiti

Summary Sequence in the Punaruu Valley, western part of Tahiti Nui, sampled to investigate field structure during reversals. All data Matuyama and younger, spanning Matuyama/Brunhes transition and upper and lower Jaramillo boundaries. Some data reproduced from Duncan (1975). 123 flows sampled with an average of 6–7 cores per flow. Natural dip of flows of 10° toward ocean. No indication of differences in stratigraphy between different sides of the river. Stepwise AF demagnetization. Non-transitional normal data are 31 Jaramillo flows, two Brunhes flows and two dykes. Jaramillo flows yield a mean VGP not significantly different from geographic axis at 95% level. Similarly for the non-transitional reverse flows. Estimate of VGP scatter identical to that of Duncan (1975) (13.8°).

Database 23 N (Jaramillo), 39 R polarity Matuyama flows.

M1652 Paleolatitudes determined from palaeomagnetic data from vertical cores

Summary Paper presents new method for determining the palaeocolatitude of a sampling site and the associated confidence limits, using inclination only data. Method is tested on data for which both inclination and declination are available: lava flows from the Pribilof Islands and Nunivak Island in the Bering Sea. Flows all of Matuyama or Brunhes age. AF demagnetization. Some directions very similar, suggesting data not independent.

Database Eight Brunhes age N records from Pribilof Isls; 13 Brunhes-age N records from Nunivak Island; eight Jaramillo-age N records from Nunivak; eight Matuyama R flows from Nunivak Isl. Care taken not to duplicate flows which are possibly not temporally independent.

PHILOSOPHICAL TRANSACTIONS OF THE ROYAL SOCIETY A MATHEMATICAL, PHYSICAL & ENGINEERING SCIENCES

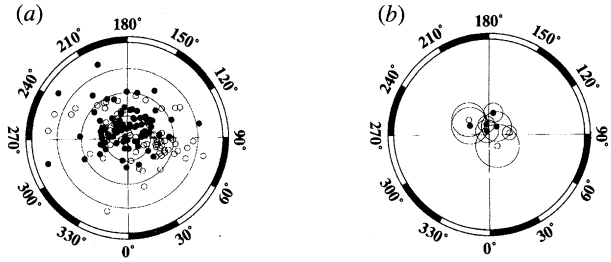

Figure 11. Africa, 86 N (normal polarity records), 80 R (reverse polarity records). All bar one of the mean VGP positions are far-sided, and all have corresponding α_{95}s less than 10°. The one near-sided mean VGP also has the largest α_{95} and corresponds to 12 Matuyama-age reversely magnetized flows from Tanzania.

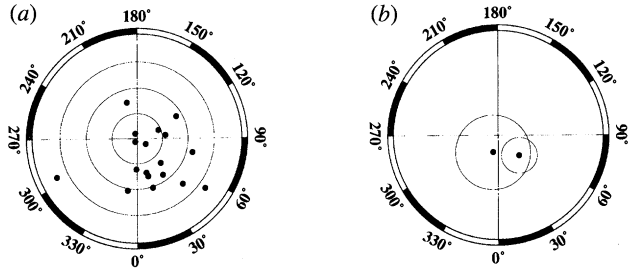

Figure 12. Antarctica, 18 N. Data are only available from two locations, both in McMurdo Province. One pole has an α_{95} of 14.8° and is markedly different from the second pole. These are the highest latitude site locations in the database, but the VGPs indicate that these data cannot provide very good constraints for PSVL studies.

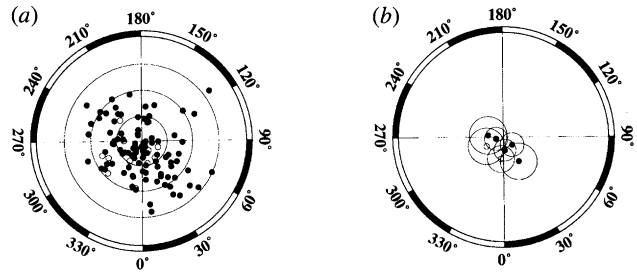

Figure 13. Asia, 100 N, 12 R. The mean VGPs are all far-sided and all have α_{95}s less than 8°. Most α_{95}s do not include the geographical north pole.

* G14-13,569,188,570,571 (M268) PSV at the Society Islands, French Polynesia

Summary PSV study involving palaeomagnetic data from five of the younger islands of the Society Islands. All samples less than 3.4 Ma. Mean VGP scatter about the geographic axis is 13.8°. Mean VGP is indistinguishable from the geographic axis at 95% confidence level. Flows mostly olivine basalts.

Database Bora Bora (3.1–3.4 Ma) – 7 N, 6 R flows Raiatea (2.3–2.5 Ma) – 8 N flows Huahine (2.3–2.6 Ma) – 7 N flows replaced from Roperch & Duncan (1990) Tahiti (0.4–1.3 Ma) – 8 N flows suitable – T1, T2, T3, T5, T6, T10, T11, T13 Moorea (1.4–1.6 Ma) – 6 R flows.

PHILOSOPHICAL TRANSACTIONS OF THE ROYAL SOCIETY A MATHEMATICAL, PHYSICAL & ENGINEERING SCIENCES

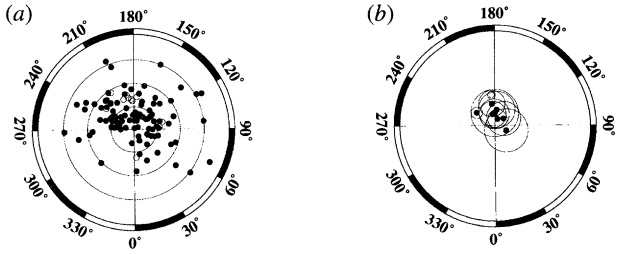

Figure 14. Atlantic Ocean, 98 N, 11 R. All except one of the mean VGPs are far sided. Typical α_{95}s are 7° and most α_{95}s just include the geographical north pole. One normal- and one reverse-polarity mean VGP have extremely small (less than 3°) α_{95}s.

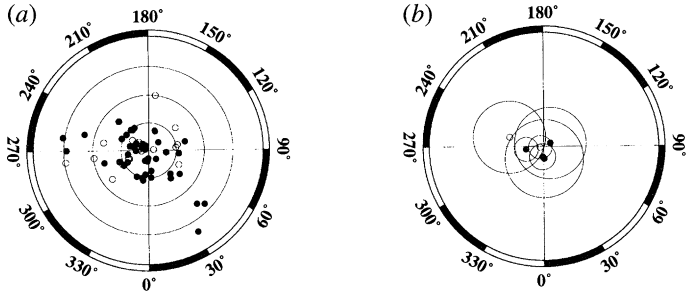

Figure 15. Australia, 46 N, 19 R. Individual flow VGPs appear to indicate far-sided effect, but there is substantial scatter and three of the mean VGPs have corresponding α_{95}s of 4° while the other three have α_{95}s of 12–15°. The large α_{95}s correspond to locations where only five records contribute to the mean direction – the temporal sampling of the data from these three locations is probably insufficient to provide good constraints on PSV in this region.

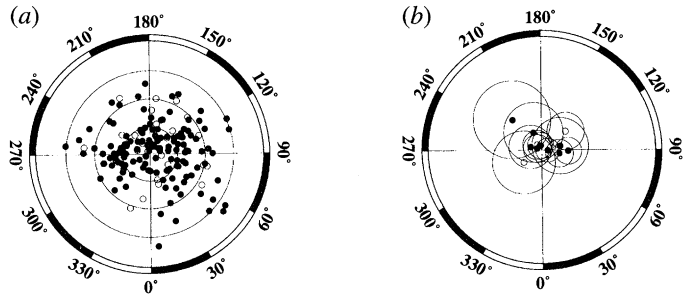

Figure 16. Europe, 138 N, 25 R. Most of the mean VGPs are far-sided and there is a large range of α_{95}s (4–14°). The largest α_{95} corresponds to five normal-polarity Brunhes-age flows from the Plateau du Velay in France. The large α_{95} corresponding to a reverse-polarity mean VGP is associated with six Hungarian flows with the only age constraint being that they fall in the 0–5 Ma range.

PHILOSOPHICAL TRANSACTIONS OF THE ROYAL SOCIETY A MATHEMATICAL, PHYSICAL & ENGINEERING SCIENCES

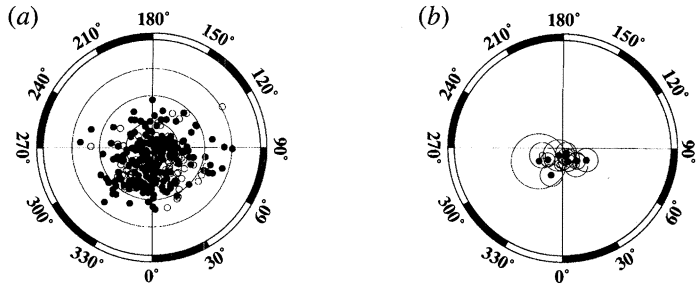

Figure 17. Hawaii, 216 N, 107 R. Hawaii contributes the second largest number of points to the database after Iceland. The individual flow data appear to exhibit far-sided VGPs, and this is confirmed by the mean VGP positions. All the mean VGPs except one have α_{95}s of 6° or less. The one exception has an α_{95} of 11° and is from seven dated Holocene flows. Low VGP dispersion in the Pacific has been noted previously (Doell & Cox 1972; Aziz-ur-Rahman & McDougall 1973; US–Japan Paleomagnetic Cooperation Program in Micronesia 1975) and the data from Hawaii in this database appears to support these observations to a first-order approximation.

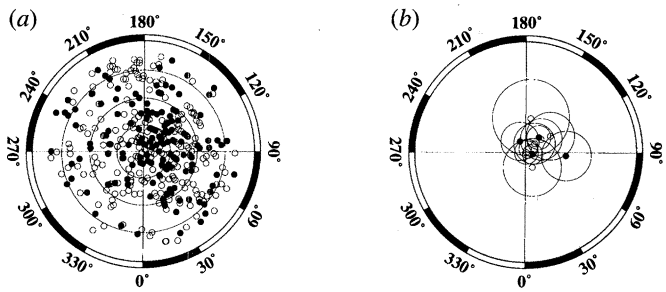

Figure 18. Iceland, 156 N, 241 R. Iceland contributes the most data to the database: nearly all the flows are of Matuyama or older age. The large number of data make it difficult to distinguish trends in the individual flow VGPs, but the mean VGPs appear to be generally far-sided. The α_{95}s are very variable, again correlating with the number of points contibuting to the mean VGP estimate. One reverse-polarity mean VGP with an α_{95} of 11° corresponds to reverse-polarity data within the Gauss normal-polarity epoch. The other reverse polarity mean VGP with a high α_{95} (14°) has just eight records contributing to the mean VGP estimate. The highest α_{95} for normal-polarity data corresponds to ten normal-polarity records with ages corresponding to the Matuyama epoch.

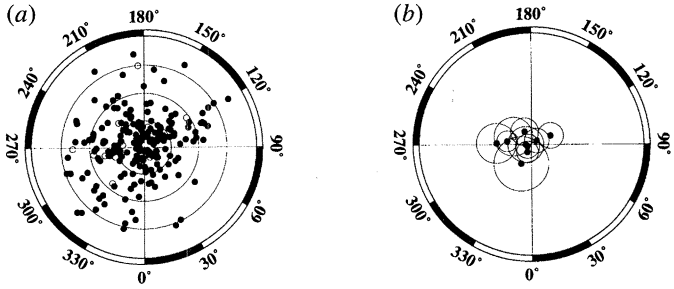

Figure 19. Indian Ocean, 200 N, 13 R. The majority of the mean VGP positions are far-sided and many have α_{95}s which do not include the geographical north pole. All the α_{95}s except one are in the range 4–7°. The one anomalous α_{95} is 10° and is associated with a moderate number of contributing flows (14) with large scatter in directions.

PHILOSOPHICAL TRANSACTIONS OF THE ROYAL SOCIETY A MATHEMATICAL, PHYSICAL & ENGINEERING SCIENCES

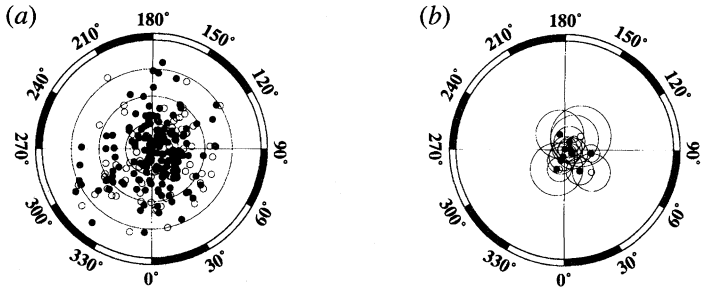

Figure 20. North America, 191 N, 72 R. North America data includes data from a very wide latitudinal band from as far south as Central Mexico up to Alaska. The data is fairly well constrained in longitude, being concentrated along the western U.S. The majority of the mean VGPs are far-sided and the α_{95}s vary from 2 to 11°, with the majority being less than 7°.

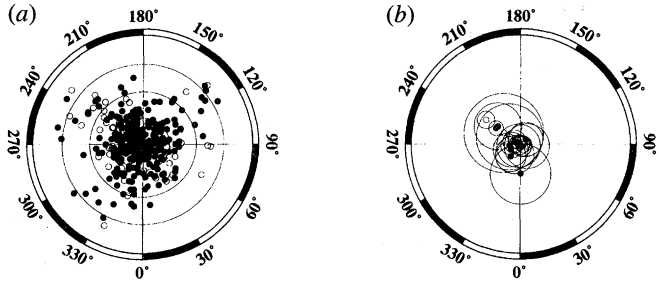

Figure 21. Pacific Ocean, 279 N, 79 R. In general, the mean VGP positions for the Pacific Ocean (excluding Hawaii) are not far-sided, in contrast to data from all the other geographical regions. Most α_{95}s are less than 7° with three being in the range 8–9°, and a further one being 11°. The largest α_{95}, 15°, corresponds to reversely magnetized data of Matuyama age from the Aleutians.

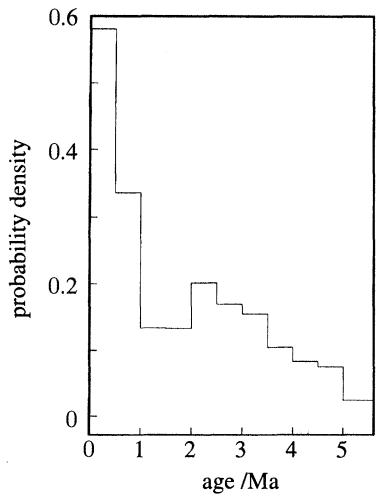

Figure 22. Age distribution of contributing data, normal and reverse polarities combined. Data from each group is assumed to be uniformly distributed over the specified age range for that group, and is then binned into 0.5 Ma bins. The normalization is such that the total area under the histogram is equal to one.

PHILOSOPHICAL TRANSACTIONS OF THE ROYAL SOCIETY A MATHEMATICAL, PHYSICAL & ENGINEERING SCIENCES

Table 2. *Data 'groups' contributing to the revised database*

(A group is defined by at least five flows within a specified age range from the same sampling area: *N* is the number of contributing flows; lat, lon are the mean site latitude and longitude; and low age, high age are the minimum and maximum ages of the contributing flows in Ma. '$' sign before reference code means that the reference is unavailable and hence no summary is provided. For abbreviations see key at end of table.)

reference	N	authors	journal	pages	lat	lon	low age	high age
			Africa					
G14-46	14	P&R 1972	GJRAS **29**	147–171	0.00	6.50	0.00	4.00
G14-52	10	Ade-Hall *et al.* 1974	CJES **11**	998–1006	27.80	17.30	0.40	2.20
G14-52	54	Ade-Hall *et al.* 1974	CJES **11**	998–1006	27.80	17.30	0.40	2.20
G13-09	12	Gromme *et al.* 1970	GJRAS **22**	101–115	−3.20	35.50	0.70	2.45
G14-21	15	P&R 1972	GJRAS **29**	147–171	4.50	9.00	0.00	0.70
G14-22	38	P&R 1972	GJRAS **29**	147–171	3.50	9.00	0.00	0.70
G14-46	14	P&R 1972	GJRAS **29**	147–171	0.00	6.50	0.00	0.70
G14-46	9	P&R 1972	GJRAS **29**	147–171	0.00	6.50	2.50	4.00
G14-46	14	P&R 1972	GJRAS **29**	147–171	0.00	6.50	0.00	4.00
			Antarctica					
G14-46	14	P&R 1972	GJRAS **29**	147–171	0.00	6.50	0.00	4.00
M1319	5	M&C 1988	JGR **93**	11 599–11 612	−77.56	166.26	0.56	1.39
M1319	13	M&C 1988	JGR **93**	11 599–11 612	−78.39	164.23	0.00	1.54
			Asia					
G14-46	14	P&R 1972	GJRAS **29**	147–171	0.00	6.50	0.00	4.00
G9-06	27	Hsu *et al.* 1966	BGSA **17**	27–81	25.30	121.50	0.01	3.40
G9-07,8	12	Hsu *et al.* 1966	BGSA **17**	27–81	23.50	121.40	0.01	5.00
M1588	35	T&H 1988	JGG **40**	221–226	35.21	138.77	0.00	0.70
C0001	5	Kono 1968	JGG **20**	353–366	35.00	139.00	0.00	1.60
C0002	8	Kono 1971	JGG **23**	1–9	35.00	139.00	0.00	1.60
G9-07,8	7	Hsu *et al.* 1966	BGSA **17**	27–81	23.60	119.50	0.01	5.00
M1301	5	McCabe *et al.* 1987	JGR **92**	555–580	14.45	120.58	0.00	5.00
$O12-262	13				43.50	143.50	0.00	1.60

P&R: Piper & Richardson. T&H: Tsunakawa & Hamano. M&C: Mankinen & Cox.

Table 2. *Cont.*

reference	N	authors	journal	pages	lat	lon	low age	high age
			Atlantic Ocean					
G14-46	14	P&R 1972	GJRAS **29**	147–171	0.00	6.50	0.00	4.00
G14-17	20	E *et al.* 1973	JGR **78**	8699–8710	38.70	−27.20	0.00	0.70
G14-31	15	A *et al.* 1974	JGG **26**	429–441	−46.90	37.80	0.00	0.70
G14-39	18	Watkins 1973	GJRAS **32**	249–267	28.20	−12.80	0.00	1.60
G14-39	10	Watkins 1973	GJRAS **32**	249–267	27.80	−18.00	0.00	1.60
G14-39	14	Watkins 1973	GJRAS **32**	249–267	28.70	−14.20	0.00	1.66
M1404	7	Schultz *et al.* 1986	EPSL **79**	208–216	−3.85	−32.40	1.70	5.10
M799	5	V&M 1974	RBdG **4**	124–132	−20.52	−29.33	2.30	3.30
M1654	9	Briden *et al.* 1979	PTRS **291**	485–527	3.30	−61.20	0.29	1.28
G14-39	6	Watkins 1973	GJRAS **32**	249–267	28.20	−12.80	0.81	1.74
M442	5	R&W 1967	Nature **215**	1470–1473	−3.85	−32.40	1.70	5.10
			Australia					
G14-46	14	P&R 1972	GJRAS **29**	147–171	0.00	6.50	0.00	4.00
G11-09	19	Cox 1969	EPSL **6**	257–267	−38.50	175.00	0.00	0.70
G13-11	17	A-ur-R 1971	GJRAS **24**	255–269	−38.00	144.50	0.00	4.50
G13-11	5	A-ur-R 1971	GJRAS **24**	255–269	−38.00	142.80	0.00	4.50
G13-11	14	A-ur-R 1971	GJRAS **24**	255–269	−38.00	144.50	0.00	4.50
G13-11	5	A-ur-R 1971	GJRAS **24**	255–269	−38.00	142.80	0.00	4.50
$G13-02	5				−4.00	150.00	0.00	0.01
			Europe					
G14-46	14	P&R 1972	GJRAS **29**	147–171	0.00	6.50	0.00	4.00
G11-12	7	Bobier 1969	CRAS **268**	20–23	45.00	3.80	0.00	2.30
G12-09	26	Doell 1970	EPSL **8**	352–362	45.71	2.99	0.00	0.70
G12-09	5	Doell 1970	EPSL **8**	352–362	44.69	4.30	0.00	0.70
G10-09	5	Sanver 1968	PEPI **1**	403–421	38.60	28.70	0.00	1.60
G10-09	5	Sanver 1968	PEPI **1**	403–421	39.50	44.00	0.00	1.60
M1072	30	K&W 1978	JG **44**	545–555	50.40	7.25	0.00	0.70
M1513	37	Bohnel *et al.* 1987	JG **62**	50–61	50.30	6.75	0.00	0.70
G11-12	13	Bobier 1969	CRAS **268**	20–23	45.00	3.80	0.70	2.41
G12-22	6	M&S-M 1970	PAG **81**	151–162	46.90	17.50	0.00	5.00
M34	6	Barberi *et al.* 1974	EPSL **22**	123–132	37.20	14.80	1.40	3.60
$O12-257	14				38.00	15.00	0.00	1.60
$G14-73	9				34.00	36.00	1.60	5.00

P&R: Piper & Richardson. E *et al.*: Ellwood *et al.* A *et al.*: Amerigian *et al.* V&M: Valencio & Mendia. R&W: Richardson & Watkins. A-ur-R: Aziz-ur-Rahman. K&W: Kohnen & Westkamper. M&S: Marton & Szalay-Marton.

PHILOSOPHICAL TRANSACTIONS OF THE ROYAL SOCIETY A MATHEMATICAL, PHYSICAL & ENGINEERING SCIENCES

Table 2. *Cont.*

reference	N	authors	journal	pages	lat	lon	low age	high age
			Hawaii					
G14-46	14	P&R 1972	GJRAS **29**	147–171	0.00	6.50	0.00	4.00
M285	28	D&C 1965	JGR **70**	3377–3405	19.50	−155.50	0.01	0.02
M285	25	D&C 1965	JGR **70**	3377–3405	19.50	−155.50	0.01	5.00
M285	29	D&C 1965	JGR **70**	3377–3405	19.50	−155.50	0.20	0.30
M667	46	Doell 1972	JGR **77**	862–876	22.00	−159.50	3.50	5.60
M31	14	Doell 1972	JGR **77**	3725–3730	23.10	−158.00	3.00	0.00
M31	11	Doell 1972	JGR **77**	3725–3730	22.00	−160.00	0.30	0.70
M42	31	D&D 1972	BGSA **84**	1217–1242	21.50	−158.10	2.40	3.60
C0003	7	Coe *et al.* 1978	JGR **83**	1740–1756	19.40	−155.50	0.00	0.02
M668	25	Doell 1972	JGR **77**	2129–2138	21.30	−157.80	0.03	0.85
M667	42	Doell 1972	JGR **77**	862–876	22.00	−159.50	3.50	5.60
M42	33	D&D 1972	BGSA **84**	1217–1242	21.50	−158.10	1.80	2.60
M31	5	Doell 1972	JGR **77**	3725–3730	22.00	−160.00	3.00	5.00
M42	27	D&D 1972	BGSA **84**	1217–1242	21.50	−158.10	2.40	3.60
			Iceland					
G14-46	14	P&R 1972	GJRAS **29**	147–171	0.00	6.50	0.00	4.00
M1496	65	K *et al.* 1980	JG **47**	31–42	64.50	−22.00	2.40	3.40
M1496	10	K *et al.* 1980	JG **47**	31–42	64.50	−22.00	1.80	2.40
M1139	52	W *et al.* 1977	GJRAS **49**	609–632	64.50	−21.50	2.40	3.40
M1139	29	W *et al.* 1977	GJRAS **49**	609–632	64.50	−21.50	3.40	5.00
G14-40	19	W *et al.* 1975	EPSL **27**	436–444	66.20	−15.20	1.09	2.00
M1496	16	K *et al.* 1980	JG **47**	31–42	64.50	−22.00	3.40	4.00
M1496	15	K *et al.* 1980	JG **47**	31–42	64.50	−22.00	2.40	3.40
M1496	103	K *et al.* 1980	JG **47**	31–42	64.50	−22.00	1.80	2.40
M1139	8	W *et al.* 1977	GJRAS **49**	609–632	64.50	−21.50	1.57	2.40
M1139	12	W *et al.* 1977	GJRAS **49**	609–632	64.50	−21.50	2.40	3.40
M1139	68	W *et al.* 1977	GJRAS **49**	609–632	64.50	−21.50	3.40	5.00

P&R: Piper & Richardson. D&C: Doell & Cox. D&D: Doell & Dalrymple. K *et al.*: Kristjansson *et al.* W *et al.*: Watkins *et al.* H&A: Hajash & Armstrong.

PHILOSOPHICAL TRANSACTIONS OF THE ROYAL SOCIETY A MATHEMATICAL, PHYSICAL & ENGINEERING SCIENCES

Table 2. *Cont.*

reference	N	authors	journal	pages	lat	lon	low age	high age
			Indian Ocean					
G14-46	14	P&R 1972	GJRAS **29**	147–171	0.00	6.50	0.00	4.00
G14-24	14	W *et al.* 1975	EPSL **24**	377–384	−38.80	77.50	0.00	0.70
G14-27	17	W 1973	JGR **78**	7763–7768	−21.10	55.50	0.00	0.70
G14-05	12	H&A 1972	EPSL **16**	231–236	−11.60	43.30	0.00	0.70
G14-23	23	H&A 1972	EPSL **16**	231–236	−12.20	44.40	0.00	1.62
G14-28	37	W *et al.* 1972	GJRAS **28**	1–25	−46.50	52.20	0.00	0.70
G14-29	32	W *et al.* 1972	GJRAS **28**	1–25	−46.50	51.70	0.00	0.70
M17	24	W&N 1973	JGR **78**	6060–6068	−37.83	77.52	0.00	0.70
C0004	27	C *et al.* 1991	JGR **96**	1981–2006	−21.00	55.50	0.00	0.98
G14-48	13	McD&W 1973	EPSL **19**	443–452	−21.00	55.50	2.00	2.11
G15-3,4,9	14	A 1971	Ph.D. thesis		−17.00	47.50	0.00	1.60
			North America					
G14-46	14	P&R 1972	GJRAS **29**	147–171	0.00	6.50	0.00	4.00
G11-08	6	D *et al.* 1969	GSAM **116**	211–248	35.90	−106.50	0.40	0.60
G14-33	30	M *et al.* 1974	G. Runds **63**	452–483	19.00	−99.00	0.00	0.70
M1429	16	B&M 1979	EPSL **42**	121–126	41.75	−121.85	0.00	0.70
M1749	20	B&N 1981	GIV **20**	235–248	19.30	−96.90	0.00	0.70
C0005	21	Steele 1985	GIV **24**	159–167	19.20	−98.60	0.00	0.70
C0006	33	M *et al.* 1986	JGR **91**	633–652	37.67	−119.00	0.00	0.75
C0007	11	H&E 1983	GJRAS **73**	39–49	58.50	−131.50	0.00	5.00
M713	9	B&S 1976	CJES **13**	547–554	62.92	−143.16	3.00	4.00
G9-13	9	Kono *et al.* 1967	JGG **19**	357–375	35.50	−111.60	3.62	4.38
C0008	13	Mankinen 1989	GRL **16**	1081–1084	38.50	−122.50	4.00	5.50
C0009	6	Heinrichs 1967	JGR **72**	3277–3294	39.25	−120.00	0.70	5.00
$G14-38	16	S&S			57.50	−130.00	0.00	5.00
$G14-38	44	S&S			57.50	−130.00	0.00	5.00
$M1316	6	Geissman			35.90	−106.50	0.00	1.60
$O11-362	23				19.60	−99.00	1.60	5.30

P&R: Piper & Richardson. D *et al.*: Doell *et al.* W&N: Watkins & Nougier. C *et al.*: Chauvin *et al.* W *et al.*: Watkins *et al.* H&A: Hajash & Armstrong. McD&W: McDougall & Watkins. A: Andriamirado. M *et al.*: Mooser *et al.* B&M: Brown & Mertzman. B&N: Bohnel & Negendank. M *et al.*: Mankinen *et al.* H&E: Hamilton & Evans. B&S: Bingham & Stone. S&S: Southier & Stone.

PHILOSOPHICAL TRANSACTIONS OF THE ROYAL SOCIETY A MATHEMATICAL, PHYSICAL & ENGINEERING SCIENCES

Table 2. *Cont.*

reference	N	authors	journal	pages	lat	lon	low age	high age
			Pacific Ocean					
G14-46	14	P&R 1972	GJRAS **29**	147–171	0.00	6.50	0.00	4.00
G14-09	23	US–Jpn CP 1975	JGG **27**	57–66	18.10	145.70	0.00	0.70
G14-35	53	B&S 1972	GJRAS **28**	317–335	53.00	−172.00	0.00	5.00
G15-14	53	I&H 1976	JGR **81**	1476–1482	−27.10	−109.20	0.00	0.70
G14-75	25	A&McD 1973	GJRAS **33**	141–155	−29.10	167.90	2.40	3.10
M663	18	Cox 1971	EPSL **11**	52–160	−0.83	−88.42	0.00	0.70
C0010	32	R&D 1990	JGR **95**	2713–2726	−16.75	−151.00	2.01	3.00
C0011	23	C *et al.* 1990	JGR **95**	2727–2752	−17.67	−149.58	0.60	1.20
C0011	23	C *et al.* 1990	JGR **95**	2727–2752	−17.67	−149.58	0.60	1.20
G14-75	12	A&McD 1973	GJRAS **33**	141–155	−29.10	167.90	2.40	3.10
G14-35	8	B&S 1972	GJRAS **28**	317–335	53.50	−168.10	1.50	2.30
M1652	8	C&G 1984	RGSP **22**	47–72	57.18	−170.36	0.00	0.80
M1652	13	C&G 1984	RGSP **22**	47–72	59.99	−165.87	0.00	0.80
M1652	8	C&G 1984	RGSP **22**	47–72	60.33	−166.09	0.80	2.40
M1652	8	C&G 1984	RGSP **22**	47–72	60.33	−166.09	0.80	2.40
G14-13,569	8	Duncan 1975	GJRAS **41**	245–254	−17.67	−149.58	0.40	1.60
G14-13,569	6	Duncan 1975	GJRAS **41**	245–254	−17.53	−149.85	1.40	1.60
G14-188,570,571	7	Duncan 1975	GJRAS **41**	245–254	−16.50	−151.27	3.10	3.40
G14-188,570,571	8	Duncan 1975	GJRAS **41**	245–254	−16.83	−151.45	2.30	2.50
G14-570,571,188	6	Duncan 1975	GJRAS **41**	245–254	−16.50	−151.27	3.10	3.40

P&R: Piper & Richardson. US–Jpn CP: US–Japan Cooperative Program. I&H: Isaacson & Heinrichs. A&McD: Aziz-ur-Rahman & McDougall. R&D: Roperch & Duncan. C *et al.*: Chauvin *et al.* C&G: Cox & Gordon. B&S: Bingham & Stone.

Reference Code is the source for the original reference and should be interpreted as follows: (*a*) GX-Y, *Geophysical Journal of the Royal Astronomical Society* Pole Compilation, pole Y in compilation X; (*b*) MX, Global Paleomagnetic Database (GPMDB) database reference code X; (*c*) OX-Y, Ottowa Pole Compilation, pole Y in compilation X; and (*d*) CX, this study reference X.

Journal reference codes are as follows:

BGSA *Bulletin of the Geological Society of America*
CJES *Canadian Journal of Earth Sciences*
CRAS *Comptes Rendues Academie Science Paris*, Series D
EPSL *Earth and Planetary Science Letters*
GIV *Geofisica Internationale*
GJRAS *Geophysical Journal of the Royal Astronomical Society*
GRL *Geophysical Research Letters*
G Runds *Geologische Rundschau*
GSAM *Geological Society of America, Memoirs*
JG *Journal of Geophysics*
JGG *Journal of Geomagnetism and Geoelectricity*
JGR *Journal of Geophysical Research*
PAG *Pure and Applied Geophysics*
PEPI *Physics of the Earth and Planetary Interiors*
PTRS *Philosophical Transactions of the Royal Society of London*
RBdG *Revista de Brasileira de Geociencias*
RGSP *Reviews of Geophysics and Space Physics.*

PHILOSOPHICAL TRANSACTIONS OF THE ROYAL SOCIETY A MATHEMATICAL, PHYSICAL & ENGINEERING SCIENCES

References

Baag, C. & Helsley, C. E. 1974 Geomagnetic secular variation model E. *J. Geophys. Res.* **79**, 4918–4922.

Barton, C. E. 1983 Analysis of palaeomagnetic time series – techniques and applications. *Geophys. Surv.* **5**, 335–368.

Barton, C. E. & McElhinny, M. W. 1981 A 10 000 year geomagnetic secular variation record from three Australian maars. *Geophys. J. R. Astr. Soc.* **67**, 465–485.

Clement, B. M. 1991 Geographical distribution of transitional VGPs: evidence for non-zonal equatorial symmetry during the Matuyama–Brunhes geomagnetic reversal. *Earth. Planet. Sci. Lett.* **104**, 48–58.

Constable, C. G. & Parker, R. L. 1988 Statistics of the geomagnetic secular variation for the past 5 Ma. *J. Geophys. Res.* **93**, 11 569–11 581.

Constable, C. 1992 Link between geomagnetic reversal paths and secular variation of the field over the past 5 Ma. *Nature* **358**, 230–233.

Cox, A. 1962 Analysis of the present geomagnetic field for comparison with paleomagnetic results. *J. Geomagn. Geoelectr.* **13**, 101–112.

Cox, A. 1968 Lengths of geomagnetic polarity intervals. *J. Geophys. Res.* **73**, 3247–3260.

Cox, A. 1970 Latitude dependence of the angular dispersion of the geomagnetic field. *Geophys. J. R. Astr. Soc.* **20**, 253–269.

Creer, K. M., Irving, E. & Nairn, A. E. M. 1959 Paleomagnetism of the great Whin sill. *Geophys. J. R. Astr. Soc.* **2**, 306–323.

Creer, K. M. 1962 The dispersion of the geomagnetic field due to secular variation and its determination for remote times from paleomagnetic data. *J. Geophys. Res.* **67**, 3461–3476.

Creer, K. M., Tucholka, P. & Barton, C. E. 1983 *Geomagnetism of baked clays and recent sediments.* Oxford: Elsevier.

Egbert, G. D. 1992 Sampling bias in VGP longitudes. *Geophys. Res. Lett.* **19**, 2353–2356.

Ellwood, B. B., Watkins, N. D. & Amerigian, C. 1973 Brunhes epoch geomagnetic secular variation on Terceira Island, Central North Atlantic. *J. Geophys. Res.* **78**, 8699–8710.

Fisher, R. 1953 Dispersion on a sphere. *Proc. R. Soc. Lond.* A **217**, 295–305.

Gubbins, D. & Kelly, P. 1993 Persistent patterns in the geomagnetic field over the past 2.5 Ma. *Nature* **365**, 829–832.

Harrison, C. G. A. 1980 Secular variation and excursions of the Earth's magnetic field. *J. Geophys. Res.* **85**, 3511–3522.

Herrero-Bervera, E., Fucugauchi, J. U., Martin Del Pozzo, A. L., Bohnel, H. & Guerrero, J. 1986 Normal amplitude Brunhes paleosecular variation at low-latitudes: a paleomagnetic record from the trans-Mexican volcanic belt. *Geophys. Res. Lett.* **13**, 1442–1445.

Irving, E. & Ward, M. A. 1964 A statistical model of the geomagnetic field. *Pure Appl. Geophys.* **57**, 47–52.

Johnson, C. L. & Constable, C. G. 1995 The time-averaged geomagnetic field as recorded by lava flows over the past 5 million years. *Geophys. J. Int.* **122**, 489–519.

Kendall, M. & Stuart, M. 1979 The advanced theory of statistics. *Inference and relationship*, vol. 2, 4th edn. New York: Macmillan.

Langereis, C. G., van Hoof, A. A. M. & Rochette, P. 1992 Longitudinal confinement of geomagnetic reversal paths as a possible sedimaentary artifact. *Nature* **358**. 226–230.

Laj, C., Mazaud, A., Weeks, R., Fuller, M. & Herrero-Bervera, E. 1991 Geomagnetic reversal paths. *Nature* **351**, 447.

Laj, C., Mazaud, A., Weeks, R., Fuller, M. & Herrero-Bervera, E. 1992 Statistical assessment of the preferred longitudinal bands for recent geomagnetic reversal records. *Geophys. Res. Lett.* **19**, 2003–2006.

Lee, S. 1983 A study of the time-averaged paleomagnetic field for the last 195 million years. Ph.D. thesis, Australian National University.

Livermore, R. A., Vine, F. J. & Smith, A. G. 1983 Plate motions and the geomagnetic field. I. Quaternary and late Tertiary. *Geophys. J. R. Astr. Soc.* **73**, 153–171.

PHILOSOPHICAL TRANSACTIONS OF THE ROYAL SOCIETY A MATHEMATICAL, PHYSICAL & ENGINEERING SCIENCES

Lock, J. & McElhinny M. W. 1991 The global paleomagnetic database. *Surv. Geophys.* **12**, 317–491.

McDougall, I., Saemundsson, K., Johannesson, H., Watkins, N. & Kristjansson, L. 1977 Extension of the geomagnetic polarity time scale to 6.5 Ma: K-Ar dating, geological and paleomagnetic study of a 3500 m lava succession in western Iceland. *Geol. Soc. Am. Bull.* **88**, 1–15.

McElhinny, M. W. & Merrill, R. T. 1975 Geomagnetic secular variation over the past 5 Ma. *Rev. Geophys. Space Phys.* **13**, 687–708.

McFadden, P. L. & McElhinny, M. W. 1984 A physical model for secular variation. *Geophys. J. R. Astr. Soc.* **78**, 809–830.

McFadden, P. L., Merrill, R. T. & McElhinny, M. W. 1988 Dipole/quadrupole family modeling of paleosecular variation. *J. Geophys. Res.* **93**, 11 583–11 588.

McFadden, P. L., Merrill, R. T., McElhinny, M. W. & Lee, S. 1991 Reversals of the earth's magnetic field and temporal variations of the dynamo families. *J. Geophys. Res.* **96**, 3923–3922.

McFadden, P. L., Barton, C. E. & Merrill, R. T. 1993 Do virtual geomagnetic poles follow preferred paths during geomagnetic reversals? *Nature* **361**, 342–344.

McWilliams, M. O., Holcomb, R. T. & Champion, D. E. 1982 Geomagnetic secular variation from C14-dated flows on Hawaii and the question of the Pacific non-dipole low. *Phil. Trans. R. Soc. Lond.* A **306**, 211–222.

Merrill, R. T. & McElhinny, M. W. 1977 Anomalies in the time averaged paleomagnetic field and their implications for the lower mantle. *Rev. Geophys. Space Phys.* **15**, 309–323.

Merrill, R. T. & McElhinny, M. W. 1983 *The Earth's magnetic field.* New York: Academic.

Merrill, R. T., McFadden, P. L. & McElhinny, M. W. 1990 Paleomagnetic tomography of the core-mantle boundary. *Phys. Earth Planet. Int.* **64**, 87–101.

Opdyke, N. D. & Henry, K. W. 1969 A test of the dipole hypothesis. *Earth Planet. Sci. Lett.* **6**, 139–151.

Quidelleur, X., Valet, J.-P., Courtillot, V. & Hulot, G. 1994 Long-term geometry of the geomagnetic field for the last 5 million years; an updated secular variation database from volcanic sequences *Geophys. Res. Lett.* **21**, 1639–1642.

Schneider, D. A. & Kent, D. V. 1990 The time-averaged paleomagnetic field. *Rev. Geophys.* **28**, 71–96.

Symons, D. T. A. & Stupavsky, M. 1974 A rational paleomagnetic stability index. *J. Geophys. Res.* **79**, 1718–1720.

Thompson, R. & Turner, G. M. 1979 British geomagnetic master curve 10 000 – 0 yr B.P. for dating European sediments. *Geophys. Res. Lett.* **6**, 249–252.

Tric, E., Laj, C., Jehanno, C., Valet, J., Kissel, C., Mazaud, A. & Iaccarino, S. 1991 High-resolution record of the Upper Olduvai transition from Po Valley (Italy) sediments: support for dipolar transition geometry? *Phys. Earth Planet. Int.* **65**, 319–336.

Valet, J. P., Tucholka, P., Courtillot, V. & Meynadier, L. 1992 Palaeomagnetic constraints on the geometry of the geomagnetic field during reversals. *Nature* **356**, 400–407.

Wilson, R. L. 1971 Dipole offset – the time averaged field over the past 25 million years. *Geophys. J. R. Astr. Soc.* **22**, 491–504.

Wilson, R. L. & McElhinny, M. W. 1974 Investigation of the large scale palaeomagnetic field over the past 25 million years. Eastward shift of the Icelandic spreading ridge. *Geophys. J. R. Astr. Soc.* **39**, 571–586.

Received 22 September 1993; revised 21 January 1994; accepted 6 May 1994